Collapse of a Black Tern (*Chlidonias niger*) Colony as a Result of Climate Change Driven Lake-Level Extremes and Anthropogenic Habitat Alteration

By

Jennifer Fuller

A thesis submitted
in partial fulfillment of the requirements
for the degree of Master of Science
(School for Environment and Sustainability)
at the University of Michigan
April 2021

Thesis Committee:

Assistant Professor Karen Alofs
Associate Professor Johannes Foufopoulos
Associate Professor Andrew Gronewold

ABSTRACT

Global climate change is expected to interact with existing environmental stressors and increasingly impact biodiversity. Great Lakes coastal wetlands and wildlife are under multiple threats including development, invasive species, and pollutants. How such stressors interact with climate-change driven, extreme lake level fluctuations to affect wildlife populations is not well understood. We investigate the rapidly declining black tern (*Chlidonias niger*) populations over a period of eight years in one of Michigan's largest colonies, at Lake St. Clair. To understand the potential drivers of these declines, we analyzed long-term hatching success data relative to both proximate ecological drivers, as well as large-scale hydrological and geospatial habitat shifts. Landcover and bathymetric data were collected using remote sensing classification and were evaluated regarding their impact on black tern population metrics via stepwise binomial general linear models. Results were then applied to land cover maps to estimate change in habitat characteristics tied to nest vulnerability. Between 2013 and 2020, the colony's breeding population and nesting success collapsed in tandem with a record rise in lake-levels. Nests with significantly lower hatching success were surrounded by deeper water, more dense, monotypic vegetation, and were located closer to the wave-exposed open area of the main lake. All these characteristics shifted unfavorably with rising lake levels, leading to progressively reduced nesting habitat availability, with a 56% reduction in hatching success and a 77% estimated decline in population size. The zone most favorable to breeding, defined by combination of interspersed native plant communities and floating nest material, was unable to shift upland as lake margins have increasingly become hardened by a combination of anthropogenic development and invasion by Phragmites australis. Subjected to progressively deeper and less stable habitat, nests have failed more frequently, likely due a combination of inclement weather and aquatic predators. Our results demonstrate that the interaction between climate change-driven lake-level rise, invasive species and coastal development are increasingly eliminating safe nesting habitat for black terns. The results also suggest that the resilience of other regional coastal wetlands needs to receive more conservation attendance in the Great Lakes region. We conclude that management must account for multiple stressors to mitigate habitat loss and protect as much wetland reserves as possible so black terns and other marsh birds can adjust to continued hydrologic extremes.

Keywords: black terns, wetland remote sensing, multi-stressors, logistic modeling

ACKNOWLEDGEMENTS

This research would not be possible without the incredible collaborative support I received over the last three years. I would like to first thank my primary advisors, Karen Alofs and Johannes Foufopoulos, for endless support, counsel, and enthusiastic, thoughtful discussion guiding this thesis to fruition. I would also like to thank Andrew Gronewold for his equally matched enthusiasm and guidance especially in the statistical analysis and coding realm. I would like to next thank Erin Rowan and Ava Landgraf for their support, amazing training, and welcoming me onto the black tern conservation team. This project would not have been possible without them connecting with me about the black terns from the very beginning.

Another thank-you goes to the Michigan Sea Grant for their generous funding through the graduate fellowship program, enabling me to continue a third year to complete this research at its full potential. Additionally, I would like to thank the American Ornithological Society, the School for Environment and Sustainability, and Rackham for additional funds which helped to fund equipment and travel required to study the black terns in the field. I would also like to thank the Michigan DNR in Harsens Island, Michigan, for providing local guidance, travel equipment, and volunteers. I would like to specifically thank my brother and volunteer, David Fuller, who was an invaluable team member during the COVID-19 pandemic restrictions. Beyond volunteering, he helped set up camera traps, took unforgettable photographs, bounced off ideas, and kept up my moral when only the two of us could work in the field. Another thanks goes to Guadalupe Cummins, a great volunteer in 2019 with an expert eye for plant identification.

Table of Contents

ABSTRACT i
ACKNOWLEDGEMENTS ii
Table of Contents iii
INTRODUCTION 1
MATERIALS AND METHODS 4
1. Study Region 4
2. Data Collection 4
a) Hatching Success 4
b) Surface Elevation & Water Depth 5
c) Geospatial Habitat Variables 5
3. Analysis 6
a) Hatching Success & Habitat 6
b) Yearly Responses to Lake Level & Habitat Change 7
RESULTS 8
1. Hatching Success & Habitat Impacts 8
2. Yearly Responses to Lake Level & Habitat Change 11
DISCUSSION 16
REFERENCES 20
APPENDIX 24
3. Head Count Estimates 24
4. Estimating Nesting Time Frame 24
5. Determining Nest Outcome 28
6. Water Depth Data Collection 29
7. Lake Level and Wind Point Locations 30
8. Imagery Preprocessing and Collection Dates 31
9. Open Lake Classification. 34
10. GLM Map Model Application 34
11. Sub-Colony change in Habitat and # Breeding Adults 34
12. Camera footage during storm events 37
13. Wind, Lake Level, and Air Temperature Fluctuation (HECWFS) 38
REFERENCES (APPENDIX) 42

INTRODUCTION

A critical step in mitigating detrimental impacts of climate change on biodiversity is accounting for interacting stressors. Examples of quantified relationships between such stressors are limited in the literature but are necessary for management to be effective and prevent greater environmental damage (*1*). Stressors are defined as factors that cause an ecosystem to experience negative effects outside the range of natural stochasticity (*2, 3*). While types of such stressors are numerous and diverse, major categories include land cover change (e.g. habitat fragmentation and loss), biological disturbance (e.g. invasive species), natural resource extraction, and pollutants (*1*, *3*, *4, 5*). Stressor interactions have been categorized as additive, synergistic (cumulatively greater stress than individually), antagonistic (mitigative), or ecologically surprising ecological surprise (cancelling or positive effect) (*6*, *7*). To understand the role of stressors, it is important to understand the ecosystem context of a study (*8*) and the fact that many stressors are likely to be exacerbated by climate change and associated extreme and/or unpredictable events (*8*, *1*).

Our study focuses on the freshwater wetlands of the Laurentian Great Lakes region of North America, cumulatively the largest body of fresh water on earth and an ecosystem of global importance (*9–11*). Broadly, freshwater wetland ecosystems are vital to maintaining global diversity and faced with an array of dynamic and interactive stressors (*12*). 95% of global wetlands are freshwater, contributing 40% of biological species, and are at heightened risk due to high freshwater interconnectivity and cumulative capacity Additionally, wetlands provide indispensable ecosystem services (e.g., freshwater supply, purification, carbon sequestration, coastal storm protection) (*12*, *13*). Great Lakes coastal wetlands are unique in that they are interconnected and tied closely with the hydrology of the largest freshwater bodies in the world (*9*). In terms of biodiversity, the Great Lakes coastal wetlands produce up to a third of the lake's primary productivity (*14*), are home to 75% of the lakes' fish species (*10*), and provide essential habitat for migratory and breeding birds (*11*). However, Great Lakes coastal wetlands are imperiled by anthropogenic stressors (e.g., invasive species, development, fragmentation, pollutants) (*12*) and <50% of their historical range remains (*15*). Invasive *Phragmites australis* and urban developments are two pervasive stressors in wetlands across the Great Lakes Basin with negative impacts on biodiversity (*16*, *17*). The specific effects of climate change, another stressor on wetlands, and its interaction with local wetland stressors are less clear. Coastal wetlands are highly adaptive to lake level shifts, where plant communities can shift their distribution lakeward or shoreward (*18*, *19*). However, climate change has been increasingly altering the Great Lakes regional water budget, resulting in periods of record-breaking lake level fluctuations. High lake temperatures and evaporation rates, in conjunction with mild winters, contributed to drought conditions from the late 1990's-2013 (*14*). This drought period was however followed by record lake level rise from 2014 until 2020, at least in part due to above-average precipitation, early snowmelt, and major ice cover events (*15*).

Here we investigate how climate change and multiple human-caused stressors interact in wetlands to impact resident wildlife populations, using as a focal organism the black tern (*Chlidonias niger*). The black tern is a small migratory shorebird and is typical of an extensive guild of other obligate marsh-nesting bird species (e.g., terns, loons, grebes, rails, bitterns). Both black terns and many other Great Lakes marsh bird species have been facing steep population losses (*19, 22–24*), with at least nine species having experienced significant losses since 1996 (*25*). Since the 1960's black tern populations have fallen by 3-8% every year (*26*), and 90% of historical Great Lakes colonies have been abandoned since 1991 (*22*). Multiple individual stressors have been associated with the decline of Great Lakes marsh birds, and our study seeks to compare their impact on black tern breeding populations.

Changes in wetland quality, size, and hydrologic dynamics can have a disproportionate effect on obligate marsh-nesting birds, including black terns (*19*)**.** A likely contributor to marsh bird habitat degradation is expansion of dense, monospecific vegetation (i.e., *Phragmites australis* or *Typha* spp.) which significantly lowers plant diversity and interspersal (*19*, *22*, *27–29*). High interspersal and diversity of plant species across different water depths is important as it increases available ecological niches, allows marsh birds to utilize different foraging and breeding strategies, and supports high marsh bird diversity (*28*, *29*). For black terns specifically, patchy vegetation provides opportunities for shelter from weather and predators, while water openings deter terrestrial predators, and facilitate takeoff, landing, and foraging access (*16*, *22, 23*, *45*, *48*, *49*)**.** Black terns appear to avoid nesting in areas of dense *Typha* spp. and *Phragmites australis* stands unless adequate patchily open areas are unavailable (*18*, *26*). It has been suggested that *Phragmites australis* and *Typha* spp. invasions are facilitated by low lake level extremes (*30*), especially in areas where native wetland vegetation is prevented by barriers from migrating lakeward (*19*) **(Figure 1)**. Invasive species establishment and human shoreline developments in turn are thought to create barriers to natural, successional migrations landward following rising water levels, though supporting literature is limited in freshwater systems (*19*) **(Figure 1)**.

Our research seeks to identify what mechanisms may drive nesting failure to better understand population trends, therefore addressing the limitations of past large-scale regional assessments in which any functional connections to reduced breeding success remained ill-defined. Few, if any, marsh bird studies address population and breeding success in the same region. Typically, shorebird population studies have focused on multiple colonies across the Great Lakes region over long periods of time, with the aim to investigate responses to landscape-level change (*11*, *22*, *25–27*, *29*, *34–36*). For the first time, our study investigates mechanisms driving population declines on multiple spatial scales, by analyzing nesting failures in one of Michigan's largest colonies over an 8-year period. As global climate change is increasingly causing lake levels to reach record highs, we evaluate how black terns respond to habitat deterioration and resulting population loss due to a combination of lake inundation and shoreward migration barriers (e.g., monotypic invasive species and coastal developments). Furthermore, we investigate how post-2017 high lake-level extremes and other stressors affect breeding success of wetland avifauna. Nest success is an obvious candidate for understanding population change mechanisms, given nests' close physical dependence on habitat structure and lake levels, with the understanding that other life history aspects may be important as well. We address the dynamic and less understood factors influencing nesting success in a coastal, as opposed to inland, wetland. Our study also covers eight years of continual lake level rise, in contrast to most previous nest success studies which have been conducted only over a few years or in relatively stable hydrologic conditions (*37–42*). At regional scales, black tern nest success has been related to vegetation patterns and water depth, which in turn are influenced by climate change and increasing anthropogenic stressors (i.e. development and invasive species). However, the directions of such effects have been inconsistent across studies (*41*). Variability in habitat and breeding relationships may reflect spatial heterogeneity in the dominant drivers of nest failure (i.e., predation, weather, abandonment), and typically short-term study periods. The long-term, environmentally dynamic, and coastal aspects of our study will provide insights not yet known to black tern breeding relationships with habitat characteristics.

We investigate black tern hatching failure and populations as a response to habitat conditions using breeding data collected between 2013 and 2020. We predicted that nests would be more likely to fail if they were in the deepest regions, surrounded by sparse vegetation, large amounts of open water, and/or closer to the larger lake. If nests were in highly dense vegetation, we hypothesized higher chance of failure due to lowered

visibility and increased difficulty for adults to take off and land. Finally, we predicted that, despite black terns' high adaptability, increasing lake levels were driving reduced success and population size.

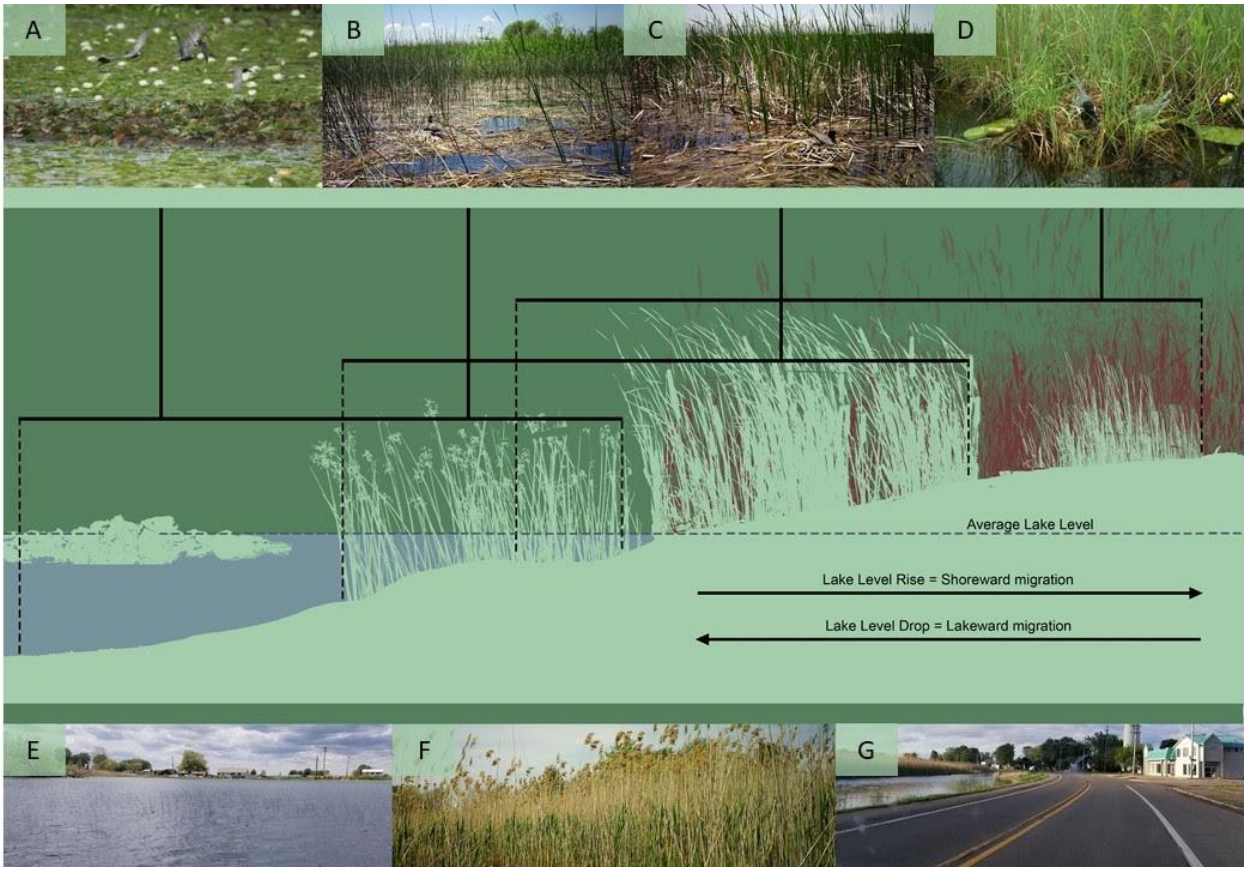

Figure 1. Graphic representation of the different vegetation zones of black tern nesting habitat in order of increasing proximity to land: (A) water lilly, (B) *Schoenoplectus* sp., (C) *Typha* spp., and (D) sedge dominant. As lake levels drop, plant communities migrate lakeward unless propagation is blocked by high hydraulic energy, boat traffic, and/or deep water (E). During drought periods and migration, shallow and exposed soil that no longer supports natural vegetation can become invaded by invasive species *Phragmites australis* and *Typha x glauca* (F, red). As lake levels rise again, communities will move up the shoreline, but can be blocked by *Phragmites australis* establishments or shoreline developments (G). Adapted from (*19, 20*).

MATERIALS AND METHODS

1. Study Region

As the largest inland freshwater delta in the world, St. Clair Flats covers roughly 101 km^2 stretched into the 1,114 km^2 Lake St. Clair. St. Clair Flats is likely a major attraction for black terns given their preference for expansive wetlands alongside bodies of open water (*32*, *33*, *41*). St. Clair Flats is historically home to one of the largest colonies of black terns in the Great Lakes Region, consisting of 137-400 breeding pairs. The capacity of St. Clair Flats to host such a large population of black terns and other species gives the region high conservation value, also reflected in its designation as a globally Important Bird Area (IBA) (*22*).

The coastal freshwater wetlands are generally dominated by native *Schoenoplectus* sp. (bulrush), *Typha* spp. (cattail), and an invasive clonal dominant, *Phragmites australis* (common reed). Invasions have been facilitated by a combination of heightened anthropogenic pressures; furthermore, invasive species establishment was likely facilitated by a period of low lake-levels (1999-2013) (*43*, *44*). Black terns build nests almost exclusively from the broken stems of emergent vegetation. Most nests sit on top of floating aggregations, or mats, of these stems, though they also frequently take advantage of logs, wood planks, or floating pieces of Styrofoam to use as a platform. In other regions, black terns also use shallow sedge tussock habitat, but there do not appear to be areas of this type of habitat supporting the St. Clair population.

2. Data Collection

a) Hatching Success

Tern breeding colonies at St. Clair Flats (SCF) (2013-2020) were monitored by no less than two volunteer and staff research technicians at least 1-2 times a week between spring migration/arrival (~May 15) and fall migration (~July 30). Monitoring colonies that were small and isolated were at times given lower priority and visited less frequently. Population sizes were estimated using records of head counts taken throughout the season at each sub-colony. Details of this procedure are in Supplementary Materials **(A1).**

Sub-colonies were initially flushed to estimate the number of nesting pairs in the area. Nests were then located by pinpointing where the adults landed after flushing and were subsequently georeferenced using a handheld GPS (2013-2016) or ArcGIS Collector App (2017-current). Researchers collected data on the dominant vegetation type(s) used for nest-construction, and on water depth measurements at each nest (when possible) using a marked PVC pole (2018-2020). The number of nests within a 30-m radius were quantified post-field season using the "near" function in ArcMap amongst nest GPS points from the same year.

Given black tern re-nesting ability, colonial nature, and high chick mobility, identifying nest survival required careful observations by field researchers and an understanding of the nest's age when possible. Except for cold-condition visits early in the season, eggs were given a "float" test to estimate clutch initiation (egg age), hatch date, and prioritize revisits for capture and banding. Records of these tests or estimated hatch dates were less consistent in early years, but this improved over time. Chick banding weight data was secondarily used to estimate their age followed by the age of the nest based on an average incubation time frame of 21-22 days. The method with the greatest accuracy was chosen for estimating a nest age if both a float test and chick weight occurred (e.g., the nest was found the day the clutch initiated, and therefore more accurate than using the chick's age-weight). Additional information on how clutch initiation was calculated is found in the Supplementary Materials **(A2)**.

Each nest was visited two to four times during the field season to determine the nest's outcome. For this work, categories of nest outcomes were combined to determine whether nest eggs either 'failed' (n = 165) or 'hatched' (n = 286, regardless of chick survival and fledging) eggs, leaving 370 nests with unknown final status See Supplementary Materials **(A3)** for a breakdown of nest outcomes. The 95% confidence interval for each year's hatching success rate was calculated with a beta distribution using the `qbeta()` function from the `'ExtDist'` package in R (*45*).

b) Surface Elevation & Water Depth

Water depth was collected and calculated using a combination of high spatial resolution bathymetry (3 m) and surface water levels from the NOAA Huron Erie Connecting Waterways Forecasting System (HECWFS) model (*20*). The bathymetric elevation (m) was determined for each nest in ArcMap using the "sample" function from the open source Lake Level Viewer Tool bathymetric map (*46*). Water depths were then estimated by subtracting the bathymetric elevation from the HECWFS surface elevation, standardized to the season onset (May 15th). Estimated water deaths were standardized to centimeters with zero set as the shallowest relative depth. The methodology for extracting the data required for this calculation is elaborated in the Supplementary Materials **(A4, A5)**.

c) Geospatial Habitat Variables

We chose geospatial habitat variables and sources based on previous literature and the resolutions of available imagery. Black terns are frequently reported to prefer habitats with a balance between open water and vegetation, vegetation percentages ranging between 25-75% (16, 22, 23, 45, 48, 49). Though from a larger spatial scale this measure is useful, it does not fully address the true habitat complexity of their breeding grounds. Not only do vegetation type and structure vary across different wetlands used by black terns, they also can vary significantly within a colony. While monitoring nests in the field in 2019 and 2020, researchers found that larger colonies were usually found in areas that contained plentiful floating, dead plant material, often secured by semi-dispersed *Typha* spp. or *Schoenoplectus* sp. Nests avoided densely packed *Typha* spp. and the highly invasive *Phragmites australis* which impede takeoff and landing, visibility, and prevent mat build-up required for nest construction. We therefore used remote sensing methods to reconstruct vegetation classes corresponding to nesting data collected over previous years. Ground truthing was used to determine that habitat structure could be generalized into four classes based on stand density: 1) dense, standing vegetation, 2) mat and scattered or cut vegetation, 3) sparse vegetation and/or sparse, scattered mat, 4) open water. Another important consideration in terms of nesting habitat is scale. The scale of habitat structure impacting the nest could be very fine, as nests are generally less than 12 inches in diameter (*47*). Previous studies have examined vegetation within a 12-m radius (31) or 2-m radius of nests (*41*), lower than available remote imagery spatial resolutions. We compared GLM p-values of hatch success in response to 3-m, a median value at 7-m, and 12-m and found that 7-m generated the strongest model results, therefore it was chosen for the final analysis.

To address the need for high-spatial resolution imagery (ideally < 1 m) covering eight years of nest monitoring, we used a combination of open-source aerial photographs from NAIP (National Agriculture Imagery Program) and purchased 4-band commercial satellite images. NDWI (normalized difference water index), which uses green and near infrared wavelengths to delineate water bodies, was chosen to capture the extent of open water (*48*). NDVI (normalized difference vegetation index) was chosen for capturing average and classified vegetation density estimates as it uses red and near infrared wavelengths to measure photosynthetic concentrations, or "greenness" (*49*, *50*).

We collected 4-band images under 1-m resolution from commercial satellites (Kompsat-2, Triplesat-3, WorldView-2 and 3), and NAIP. We chose 1-m resolution images within nine days of each other (standard deviation = 8.71 days) between late June and July to prevent as much timing differences during annual growth seasons as possible. We obtained 5-m resolution imagery (Rapideye-5 and PlanetScope) through Planet Images to capture more general, average NDVI values. With the advantage of higher temporal resolution, images from Planet could be collected for each year during the breeding season, allowing anniversary dates to be interpolated. All images were resampled to 1- or 5-m resolution depending on their source, and geometrically, radiometrically, and atmospherically corrected based on their individual requirements. Imagery preprocessing methods, image dates, and resolutions are detailed in the Supplementary Materials **(A6).**

Mean NDVI was sampled from each nest's 7-m radius buffer region from linearly interpolated anniversary images (PlanetScope and Rapideye-5, 5-m resolution). Extraction used the Zonal Statistics 2 toolbox which is capable of handling overlapping polygons. Open water was classified using Natural Breaks (Jenks) Unsupervised Classification on NDWI raster images from yearly 1-m resolution images. Island developments or regions not considered wetland were heads-up digitized using 1-m resolution NAIP imagery from 2014, 2016, and 2018. The open water and island development classes were used to mask 1-m NDVI raster images and generate three vegetation classes using the Iso Cluster Unsupervised Classification tool in ArcMap. The percentage of each class was then sampled within each 7-m radius nest buffer using the Tabulate Intersection Tool. Because there was no available high-resolution imagery in 2015, the percentage of habitat classes surrounding nests were estimated by averaging measured values from classified 2014 and 2016 maps. To measure potential impacts of proximity to the housing developments, any open water, and the larger body of open water (Lake St. Clair), distance values were extracted from the digitized developed regions, the open water class, and a "main lake" delineation using the "near" function in ArcMap. The "main lake" variable was created for each year by delineating the outer edge of the open water class to remove any inundated regions surrounded completely by vegetation. The Supplementary Materials provide further information on the methodology for the "main lake" classification **(A7).**

3. Analysis

a) Hatching Success & Habitat

The relationships between hatching success and habitat variables were analyzed using R version 4.0.3 (*45*). A multiple logistic regression with a binomial (logit-link) fit using the `glm()` function from the `'stats'` package in R (*45*) to determine the influence of habitat and biological predictors on nesting survival. The following 10 habitat or biological variables were examined in the analysis as fixed effects: (1) relative, initial water depth (cm), (2) distance to housing developments (m), (3) distance to the main lake (m), (4) distance to any open water (m), (5) percentage of open water within a 7-m radius, (6) percentage of dense vegetation within a 7-m radius, (7) percentage of medium vegetation within a 7-m radius, (8) percentage of sparse vegetation within a 7-m radius, (8) estimated start of incubation as the number of days before or after May 15th of each year, (9) mean NDVI within a 7-m radius, (10) number of nests within a 30-m radius. Continuous habitat variables were first checked for multicollinearity using a Pearson correlation test using the `cor()` function from the `'DescTools'` package in R (*45*). No r_s values were greater than 0.6 and all predictors were retained.

To compare model coefficients, all continuous independent variables were normalized using the `scale()` function of the `'base'` package in R (*45*) which computes a z-score for each variable using its mean and standard deviation. Models were compared using stepwise selection in both directions using the `step()`

function from the 'stats' package c To determine the best explanation of the data variation, each model was assessed for the lowest Akaike's information criterion (AIC) (*51*). A Receiver Operator Curve (ROC) and AUC (area under the curve) was generated using the `roc()` function from the 'pROC' package in R c to measure the best model's predictive performance (*51*).

b) Yearly Responses to Lake Level & Habitat Change

To visualize the geographic extent of the habitat's potential to predispose nests' vulnerability, the coefficients and intercept from our selected GLM were applied to raster layers in ArcMap using the Raster Calculator Tool (see Supplementary Materials **A8** for background methodology). For spatial projections, the biological variable describing clutch initiation date was removed. The remaining geospatial variables and associated raster layers were rescaled using min-max feature scaling. The raster calculations generated a final model describing nest failure probability on a scale of 0 to 1. This model's performance was also assessed using an ROC (Receiver Operator Curve) plot (52) and AUC (area under the curve) using the `roc()` function from the 'pROC' package in R (*45*).

The final maps were then masked to exclude regions that were determined *a priori* to be unsuitable for nesting. This includes developed or dry-land islands and peninsulas, open water, and areas where vegetation within a 7-m radius breached an NDVI value of 0.72. Specifically, 0.72 was the maximum NDVI surrounding a known nest and it is assumed that the likelihood of any nest existing within areas with any higher value is extremely low. This was also confirmed by extensive nest searching in the field, which determined that nests are not built within dense monocultures of *Phragmites australis* or *Typha* spp. This is because the vegetation mats required for nesting do not accumulate among stands when the vegetation grows too closely together; furthermore, nesting birds are unable to take off or land.

To quantify sub-colony breeding pair population size and their response to changes in sub-colony habitat in the geospatial model, we applied a general linear mixed model (GLMM) using the `lmer()` function from the 'lme4' package in R (*45*). Predictor variables were chosen *a priori*, and included the area of open water, uninhabitable vegetation (NDVI>0.72), any habitable area, and area with >50% hatch success. The area of classified predictor variables per sub-colony were extracted from the geospatial model outputs in ArcMap. The response variable, i.e., the number of maximum breeding pairs per sub-colony, as well as the predictor variables were scaled using the `scale()` function from the 'base' package in R (*45*) prior to running the GLM, to account for considerable differences in measurement units. The area with >50% hatch probability and any habitable area were correlated, as was uninhabitable vegetation and open water extent. The selected model was chosen based on having the highest R^2 and including the most significant predictors. After evaluating all possible variable combinations, the selected model included the area with >50% hatch probability and uninhabitable vegetation. Summary tables by each individual sub-colony, year, and habitat category can be found in the Supplementary Materials **(A9).**

RESULTS

1. Hatching Success & Habitat Impacts

We compiled eight years of hatch rates and population counts in the St. Clair Flats region to review how both have changed between 2013 and 2020. During this timeframe, Lake St. Clair's average May-July lake level (during the black tern breeding season) rose by 1.03 m as the result of regional changes in climate (*20*) **(Figure 4)**. Hatch rate (percentage of hatched nests out of nests of known status), dropped by 56% between 2013 (90%) and 2020 (35%) **(Figure 2)**. Corresponding to this decline in hatch rate, the monitored population of black terns at Lake St. Clair Flats dropped by 77% since 2013 **(Figure 2, Table 1)**.

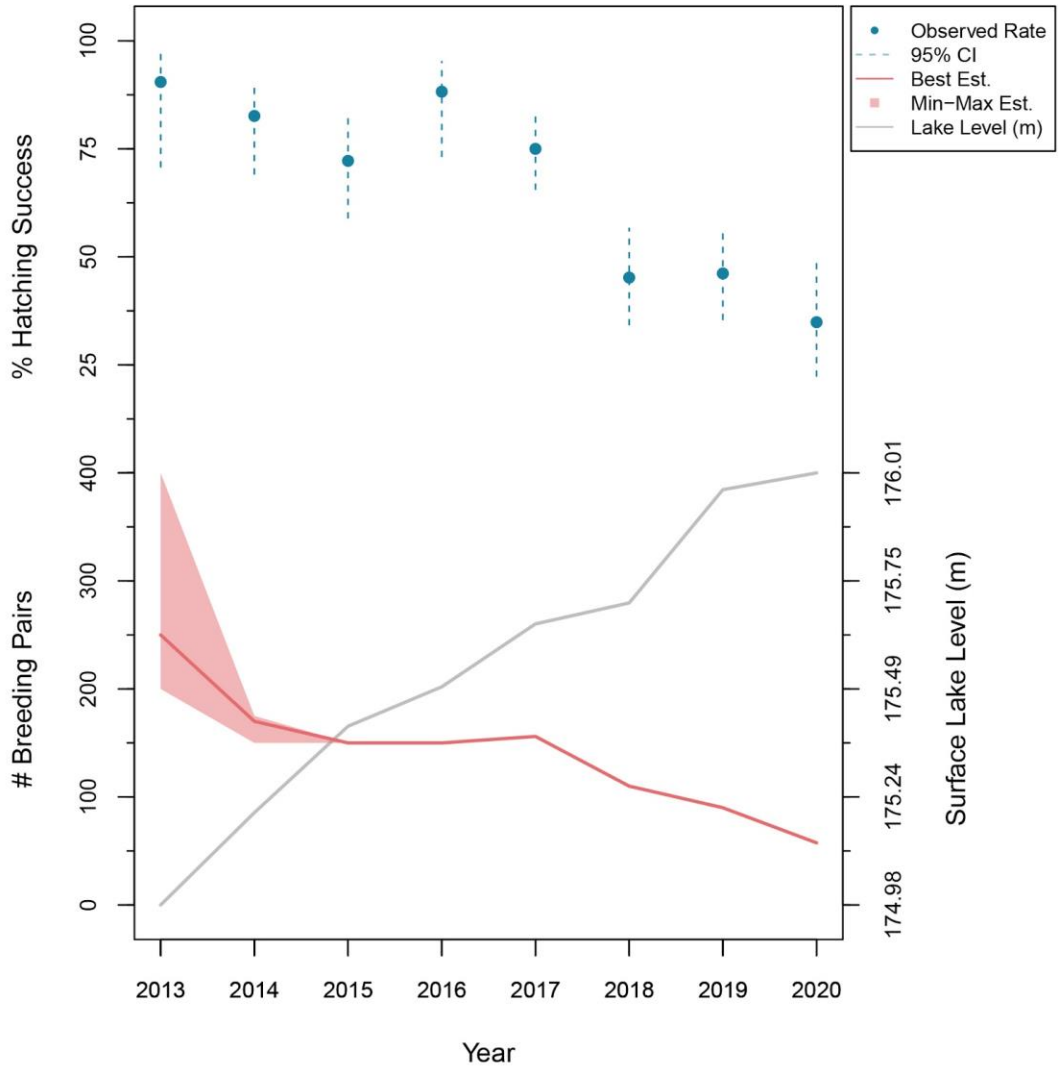

Figure 2. Yearly estimated number of black tern breeding pairs across St. Clair Flats (solid red line, right y-axis), average surface lake level (May-July) (m), and yearly hatching success rates (% hatched of total nests and 95% confidence intervals (CI), dots and whiskers, left y-axis). Population size is a "best" estimate of individuals, with maximum and minimums (shown by shaded sections) recorded in 2013

Field investigation of hatching failures revealed several causes. 40% of nests disappeared completely between two censuses, while 7% of had eggs missing from an otherwise intact nest. Known destruction by weather events accounted for 16% of complete failures. 4% of nests were abandoned and had perished eggs, or chicks. The remaining nests had an undetermined cause of failure. A binomial (logit-link function) Generalized Linear Model (GLM) was used to compare habitat variables, the number of other black tern nests in a 30-m radius, and clutch initiation, between 234 hatched nests and 124 failed **(Table 1)**. Habitat variables in the final model selected included 1) lake distance (nest to the unvegetated St. Clair Flats River Delta), 2) house distance (nest to developed land), 3) open water distance (nest to any open water patch), 4) mean NDVI (surrounding average Normalized Difference Vegetation Index (NDVI) (*30*) 5) % dense vegetation surrounding the nest (i.e. amount of the densest surrounding vegetation).

Stepwise regression procedure **(Table 1)** identified the model selected **(Table 1, Table 2)**. The estimated clutch initiation timing percentage of dense vegetation, relative nest water depth, and lake distance were statistically significant (alpha<0.05). Mean NDVI and house distance were not significant, but collectively improved the AIC and AUC of the model **(Table 1)**.

Table 1. Summary of stepwise regression process for identifying the selected model (2, green) of hatch probability in response to habitat and biological predictors. Model steps include the initial null model (all predictors) and subsequent steps with coinciding AIC, Δ AIC (< 2.0), and AUC.

Predictors	Model Steps			
	NULL	1	2	3
Relative water depth	0.037	0.042	0.029	0.032
Lake distance	0.032	0.032	0.032	0.014
% Dense vegetation	0.880		3.19E-04	2.85E-04
Clutch initiation day	3.58E-04	3.46E-04	1.63E-04	2.91E-04
Mean NDVI	0.084	0.090	0.170	0.145
House distance	0.120	0.104	0.087	
% Medium vegetation	0.793	0.001		
% Sparse vegetation	0.786	0.004		
% Open water	0.762	0.008		
Open water distance	0.598			
# Nests (30-m radius)	0.795			
AIC	420.21	414.59	411.71	412.68
Δ AIC		2.88	0	0.97
AUC	0.7583	0.7568	0.7555	0.7495

Table 2. Summary table of the selected (see Table 1.) binomial GLM results to predict hatching success in response to habitat variables and clutch initiation covariate. Includes variable coefficients, standard error (SE), z score (Z), and p-value (P).

Hatching Success Binomial Generalized Linear Model (logit-link)				
Predictor	**Coefficient**	**SE**	**Z**	**P**
Clutch initiation	-0.454	0.120	-3.770	<0.001
% Dense vegetation	-0.515	0.143	-3.599	<0.001
Lake distance	0.347	0.162	2.146	0.032
Relative nest water depth	-0.307	0.141	-2.178	0.029
Mean NDVI	0.200	0.146	1.371	0.170
House distance	0.215	0.126	1.713	0.087

Hatching success was negatively correlated to the date of clutch initiation, relative nest water depth, and the percentage of dense vegetation surrounding a nest in a 7-m radius, and positively to distance from the lake **(Table 2, Figure 3)**. Hatching success was positively related to house distance and mean NDVI, **(Table 2, Figure 3)** but were not statistically significant in any of the top seven models.

Hatch likelihood declined the later the clutch was initiated, where a nest was 0.64 times more likely to fail per day later into the season. Increasing amount of dense *Phragmites australis* around a nest negatively impacted nest success. The average percentage of dense vegetation (consisting mostly of dense *Phragmites australis* or *Typha* spp.), and classified as exhibiting the highest relative normalized difference vegetation index (NDVI) (*30*) surrounding a nest's 7-m radius was lower by 18% in hatched versus in failed nests (5% vs. 23%). Excluding outliers outside 1.5 times the interquartile range, the maximum percent cover of dense vegetation for hatched nests was no greater than 58%, whereas the maximum for failed nests reached 98%. Relative nest water depths were on average 0.098 m shallower in hatched nests than those that failed. Hatched nests were found to have a mean distance from the open water of the main lake of 22.44 m, while failed nests were significantly closer (12.32 m). Though distance to land and human developments was not a statistically significant predictor of hatching success, more successful nests were on average 45 m further away from developments. Differences in mean NDVI between successful and failed nests were minimal and not significant.

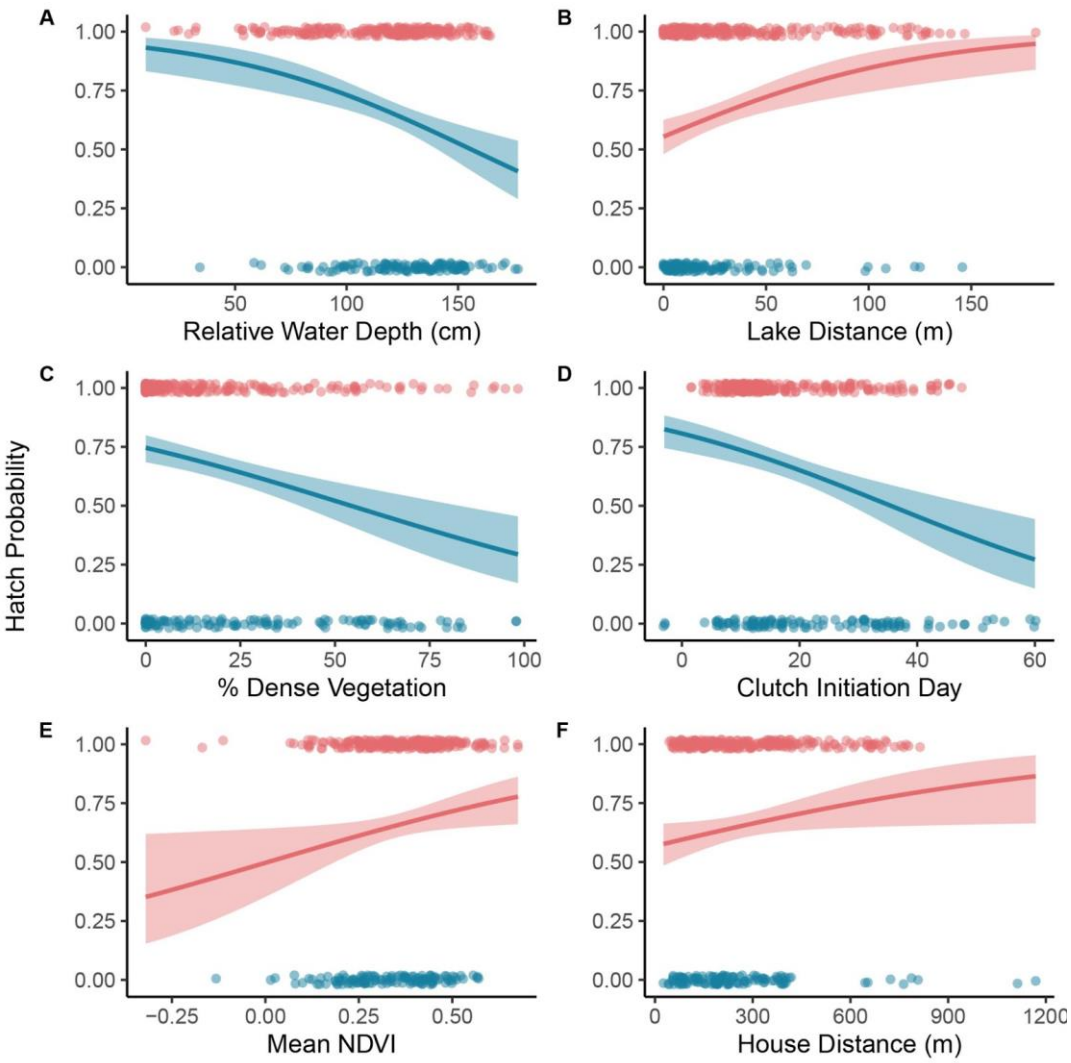

Figure 3. Hatching success probability and 95% confidence intervals with respect to individual variables (A-F) included in the two top binomial general linear models. These include: A. Clutch initiation day (# days after May 15th), B. Percentage of surrounding dense vegetation in a 7-m radius, C. Relative nest water depth (cm), D. Distance to the open water of the main lake (m), E. Distance to developed land (housing) (m), F. and the average NDVI in a 7-m radius.

2. Yearly Responses to Lake Level & Habitat Change

We plotted all habitat variables and clutch initiation dates included in the GLM, against yearly average May-July lake levels (*20*) **(Figure 3)**. Average relative nest water depth increased steadily as annual lake levels rose. Average nest distance to the open lake water fluctuated between years without showing particular trends. Extent of dense vegetation remained consistently low until 2017 when the lake level reached a height of 175.65 m above sea level (asl.) and birds were forced to shift their nests into denser, less favorable vegetation. Clutch initiation dates did not show any significant trends with increasing lake level, apart from the last two study years when start dates appeared to extend substantially later into the summer season. Both average NDVI and average nest distance to houses did not vary in a predictable manner over the course of the years.

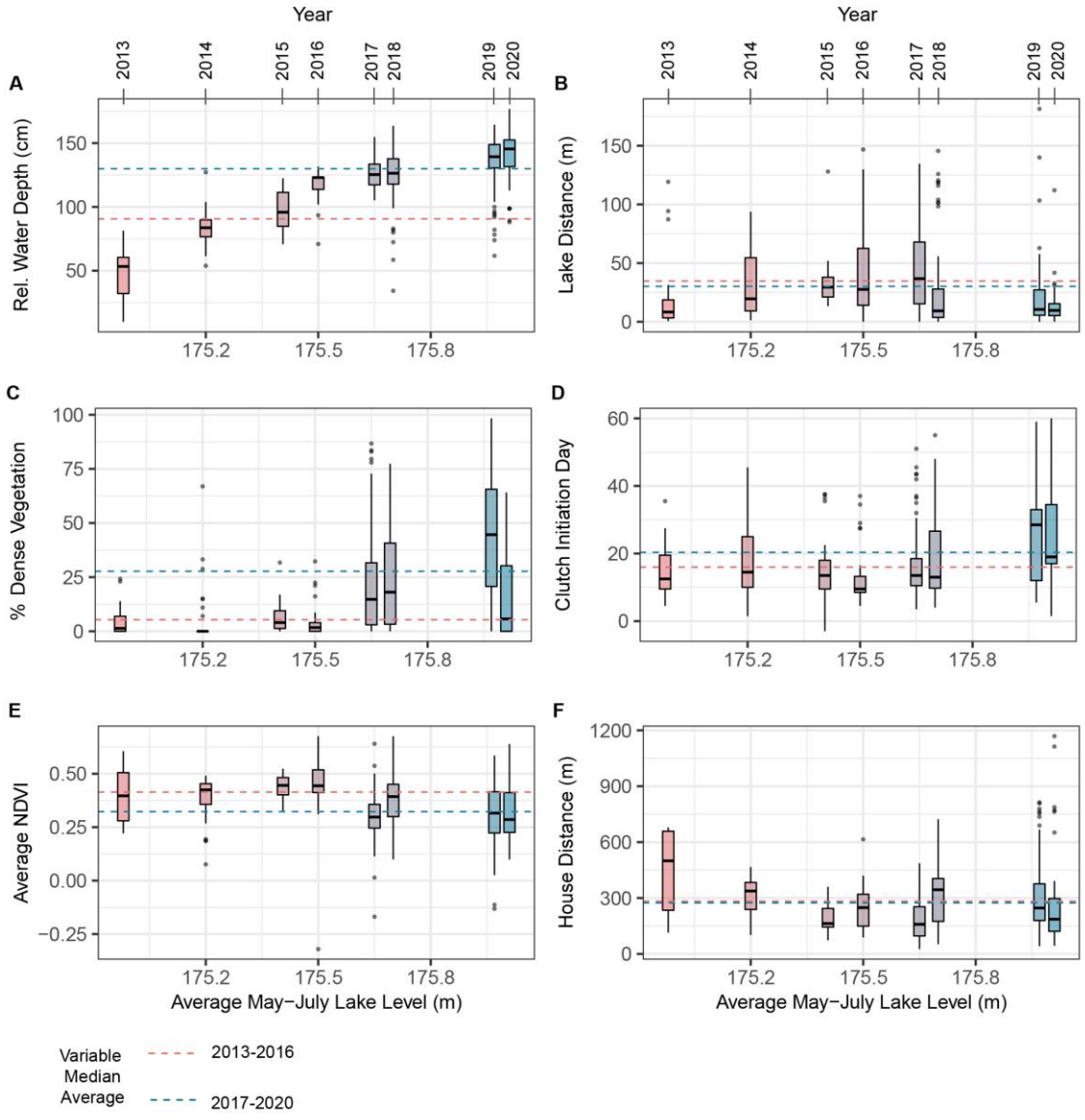

Figure 4. Boxplots of the nest variables included in the final GLM, against the respective average May-July surface lake level. Lake levels increased nearly monotonically over the course of the study. The average median for values from 2013-2016 (red) and 2017-2020 (blue) are plotted as horizontal dashed lines for reference.

To spatially map how conditions determining hatching success changed over the years, we modified the best AIC model by excluding non-spatial variables (i.e., clutch initiation date). The AIC of this model increased from the original model to 424.34 and the AUC declined slightly to 71.72%, which is expected with the removal of clutch initiation. Statistically significant variables in the spatial model were the same as in the previous models **(Table 3).** NDVI and house distance were retained in the spatial model mapping hatch probability as they still improved both the AIC and model performance (AUC).

Table 3. Summary table of geospatial GLM used to predict and map hatching success in response to habitat variables. Includes variable coefficients, standard error (SE), z score (Z), and p-value (P).

Geospatial Hatching Success Binomial Generalized Linear Model (logit-link)				
Predictor	**Coefficient**	**SE**	**Z**	**P**
(Intercept)	2.769	2.486	1.114	0.265
% Dense vegetation	-0.019	0.005	-3.637	<0.001
Relative nest water depth	-0.113	0.049	-2.329	0.020
Lake distance	0.022	0.009	2.568	0.010
House distance	0.014	0.010	1.366	0.172
Mean NDVI	0.031	0.020	1.549	0.121

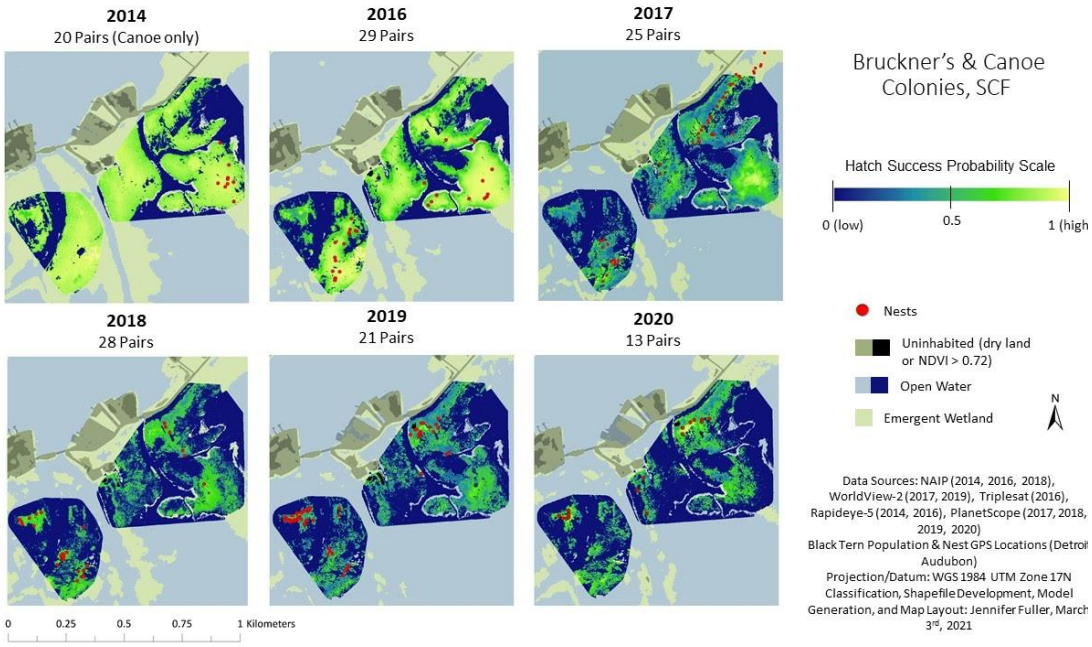

Figure 5. Decline in tern habitat nesting quality in the study area over the years. Mapped nesting quality is based on the applied binomial GLM output for hatching success as based on geospatial habitat variables (Water depth, Distance to lake & housing, % of surrounding dense vegetation, and mean NDVI). All study years are shown except 2013 (no nest searches) and 2015 (no available imagery). Only those areas for which quality imagery was available for all years have been mapped in detail (inside of two polygons). Water is shown in shades of blue, while land is shown in shades of tan. Emergent wetland, the tern's nesting habitat, is shown in shades of green ranging from light yellow-green (associated with high nesting success) to green-blue (low nesting success). Nests are shown as red circles. Images show examples of two of the 13 sub-colonies in the study area; Bruckner's (left) and Canoe (right). Bruckner's sub-colony was not searched in 2014. While rising lake levels lead to a pronounced reduction of emergent wetlands, shorelines hardened through human activities (roads, dams, build structures) prevent the establishment of new shoreward wetland areas.

We examined whether the decreases in the amount of available nesting habitat were related to the number of breeding pairs within respective sub-colonies using sub-colony geospatial visualization. The relationship between sub-colony population and habitat category was further quantified using a general linear mixed model (GLMM). The example in **Figure 5** represents two of 13 individual sub-colonies used in the general linear mixed model (GLMM) **(Table 4)**. **Figure 6** illustrates the results of GLMM, i.e., sub-colony population size as a response to changes in two major wetland categories derived from the spatial model, specifically pertaining to black tern hatch probability or habitability.

To investigate the relationship between habitat availability and population size, we used a general linear mixed model (GLMM) including the maximum breeding pairs at 13 sub-colonies between 2013 and 2020. The number of breeding pairs was significantly related to the subcolony's area with >50% hatch probability ($p<0.001$) **(Table 4, Figure 6A)**. Area of uninhabitable vegetation was not a significant predictor of the number of sub-colony breeding pairs, though it improved the model's marginal and conditional R^2 (0.331, 0.426, consecutively) from one only including area with >50% hatch probability **(Table 4)**.

Table 4. Summary table of the general linear mixed model (GLMM) predicting the response of breeding pairs by changes in area of 2 major wetland classes: >50% hatch probability and uninhabitable vegetated regions. Includes predictor coefficients, confidence intervals (CI), and p-values (P). Random effects include the variance from the mean (σ^2), between-subjects-variance ($\tau_{00\ subcolony}$), interclass correlation coefficient (ICC), and number of sub-colonies sampled (N). Number of observations and variance explained by fixed effects (Marginal) and fixed and random effects (Conditional) R^2 are also reported.

	Effects of Landcover Area (m^2) on # Breeding Pairs		
Predictor	**Coefficient**	**CI**	**P**
(Intercept)	-0.01	-0.29 - 0.27	0.948
Area with >50% Hatch Probability (scaled)	0.6	0.35 - 0.85	<0.001
Area of Uninhabitable Vegetation (scaled)	-0.2	-0.46 - 0.06	0.134
Random Effects			
σ^2	0.61		
$\tau_{00\ subcolony}$	0.1		
ICC	0.14		
$N_{\ subcolony}$	13		
Observations	49		
Marginal R^2	0.331		

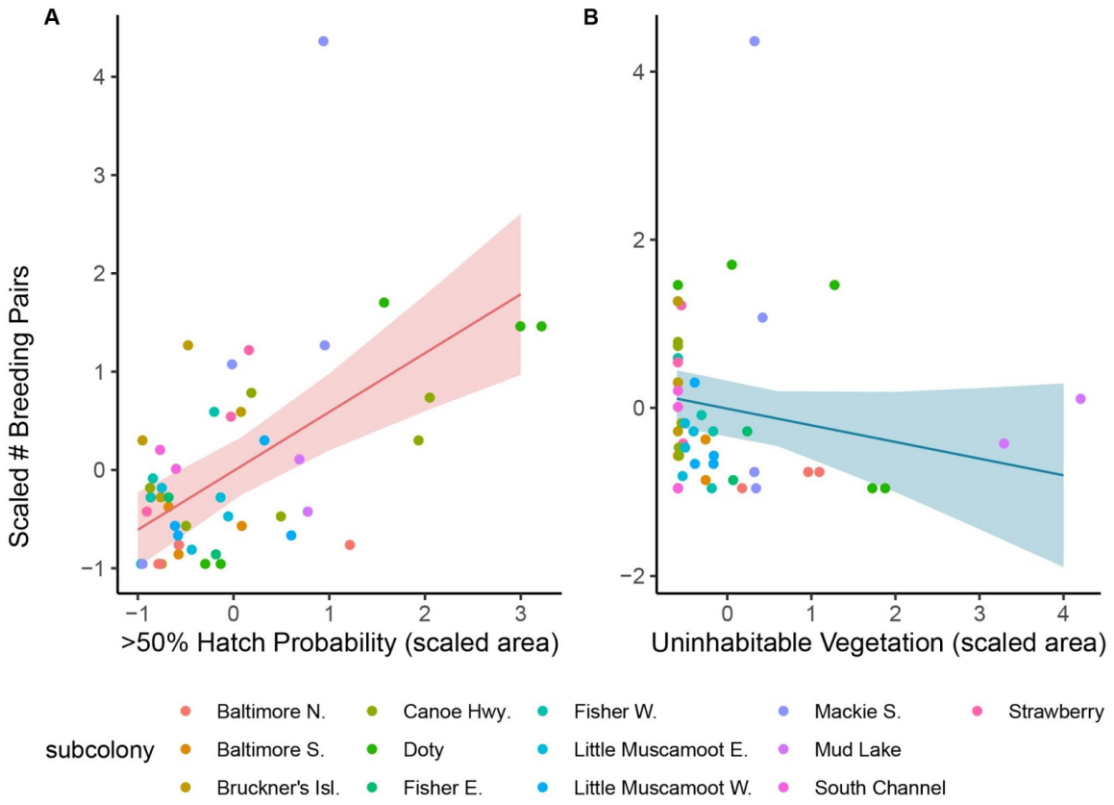

Figure 6. General linear mixed model (GLMM) plots predicting the response of breeding pairs by changes in area of 2 major wetland classes: >50% hatch probability (A) and uninhabitable vegetated regions (B). Colored points denote scaled number of breeding pairs versus the scaled area of each class. Model estimates and 95% confidence intervals are represented by the solid line and filled area, consecutively.

DISCUSSION

The goal of this study was to examine how climate-driven lake level change interacts with other anthropogenic stressors to impact wetland biodiversity and in particular black terns, an archetypical shorebird species. For the first time, we explicitly identify the hazardous nesting conditions in a freshwater coastal wetland, which include deeper water at the nest, closer proximity to the open water area of the main lake, and more dense surrounding vegetation. We then show how most of these hazardous nesting conditions have been exacerbated in recent years by rising lake levels. Our results indicate that black terns in coastal wetlands, and likely other marsh birds, rely on a patchily vegetated zone with intermediate depths between the deepest, vegetation-free open lake, and shoreward dry land. Under natural conditions, Lake St. Clair's coastal transition zone is dominated by interspersed open water, reed mat, *Typha* spp. and *Schoenoplectus* sp. and can maintain its extent by shifting shoreward or lakeward depending on rising or falling lake levels. The dynamic adjustment of coastal wetlands appears to be increasingly inhibited by immovable coastal barriers including human developments (e.g., housing, roads, seawalls, channels) and establishments of invasive monospecific vegetation (e.g., *Phragmites australis*, *Typha x glauca*). In conjunction with regional lake-level rise, immobile shoreline barriers have been reducing the available nesting habitat for black terns and have resulted in a dramatic decline in black tern hatching success and population size.

To explain the decline of black tern populations observed over large, regional spatial scales, it is important to consider the individual factors influencing nesting success. We found that earlier clutch initiation date was the strongest factor associated with improved nesting success. This mirrors previous findings both in black terns (*37*)**,** and in other, seasonally breeding birds in general (*53*, *54*). While the timing of clutch initiation was not strongly related to lake-levels, nests in 2019 exhibited considerably later initiation dates and the last two years exhibited the highest standard deviations. Reduced availability of high-quality nesting habitat due to high water levels could increase nesting site competition and the time required to locate suitable habitat for nesting. Late-season renesting attempts may also have grown more frequent as habitat conditions became more hazardous and nest failure rates increased.

In addition to the timing of clutch initiation, the percentage of surrounding habitat in the densest vegetation category was the next strongest predictor of hatching success. Our ground-truthing observations found that the dense wetland vegetation class is typically dominated by monospecific stands of *Phragmites australis* and *Typha* spp. Black terns are well-known to prefer patchier mosaics of standing vegetation and open water, which provide spaces for take-off and landing, and improved foraging access (*41*). Therefore, it is not surprising that monospecific stands have a negative effect on rates of hatching success. Aside from forming dense stands, *Phragmites australis* grows exceptionally tall (up to 4.6 m in height) (*55*) and can diminish nest visibility and the ability of adults to detect and ward off predators. Lack of visibility is especially problematic if both adults are disturbed, as black terns will frequently and collectively mob intruders near the sub-colony, even if it is not relatively close to their own nest (*40*, *56*). Our data indicate that declining availability of quality nesting sites is increasingly forcing the black terns of St. Clair Flats, especially during the last few years of the study, to nest in largely unsuitable dense invasive vegetation stands. An alternative or complementary interpretation could be that there is an underlying positive relationship with available nesting material. Unfortunately, we did not have a reliable method of specifically capturing the extent of floating mats using 4-band imagery, but we observed that densely packed *Phragmites australis* and *Typha* spp. stands block out floating mats entirely. It is therefore reasonable to assume that the dense vegetation class represents an antithesis of available nesting material. The mix of medium and sparse vegetation and open water may

support an unknown, but likely important quantity of floating mat required for nest-building, stability, and protection from aquatic predators.

Hydrology was a critical factor shaping hatching success, acting through multiple pathways, including relative nest water depth at nest locations, as well as distance of the nests from the open water of the main lake. In contrast to the Lake St. Clair river delta (referred to as the "main lake"), the coastal wetlands are shallower, have reduced fetch, and are characterized by emergent vegetation buffers which provide crucial protection from wind and wave action (*57*). Deeper water within wetlands, however, is still capable of permitting higher energy currents and larger waves during storms and seiches, and attenuates emergent vegetation density that is needed to reduce wave action (*19*, *57*). Black tern nests in Lake St. Clair are buoyant but minimally constructed, and their interlocked, floating vegetation stems are susceptible to breakage by wind and waves. Therefore, *Schoenoplectus* sp. and *Typha* spp. stands provide a critically important web of physical barriers which maintain dense, stable floating mats for nesting. This was confirmed by field observations of how proximity to the open lake and deeper waters allowed for more current, wave and wind action which contributed to the attenuation of protective barriers and the loss of floating mat habitat. Though few studies of black tern nest success have found a relationship to water depth, nests in a British Columbia colony were more likely to fail by rising water, wind and waves, if they were surrounded by less standing vegetation (*38*). In 2020, nesting mats surrounded by substantial emergent vegetation withstood multiple storms on camera traps, while one nest which was exposed to open water on one side was destroyed by wave action during a storm event between June 10th and 11th (see Supplementary Materials **A10** for images) when lake levels rose 0.06 m with wind speeds up to 17.12 km/h (*20*).

Aquatic predators represent another important nesting hazard that may worsen with deeper waters and with increasing proximity to the main lake. Deep water and closer lake access likely increase visibility and accessibility of nests to predators. The main species capable of preying eggs and chicks in Lake St. Clair are muskellunge and northern pike which originate from cooler, deeper regions of open water, especially in the warmer months during black tern breeding season (*58*, *59*). Muskellunge are strongly associated with emergent vegetation (mainly consisting of *Schoenoplectus* sp. and floating mats) which black terns use for nesting. Muskellunge have also been commonly found in depths between 0.75 and 0.95 m (*53*) overlapping broadly with the depths (0.7-1m) of the nests with highest failure rates. Northern pike and largemouth bass may also be potential nest predators, though they are reported to more frequently use denser submerged vegetation and deeper habitats (*58*, *59*). Predator-related failures of black tern nests have not been well documented due to the difficulty of capturing an event on camera or in person. However, multiple eggs in Lake St Clair Flats have been found with puncture marks (indicating water snake (*Nerodia sipedon*) encounters), and one chick was observed eaten by an unknown fish species in 2020 (Erin Rowan, pers. comm.). Due to their fragile nature, tern nests are also in danger from non-predatory fish. Fish spawning or feeding activity by large fish can lead to the destruction of floating mats and nests. Common carp frequent the coastal wetlands in Lake St. Clair and are known to form spawning aggregations in nearshore aquatic and submersed vegetation between May and June (*60*). During the months of May through July, common carp have been tracked in average depths between 1.6-3.3 m (*60*), and are well known to physically damage submergent vegetation (*61*). Common carp were frequently observed breaking apart floating mats on the water surface, most frequently in the South Channel sub-colony.

Our geospatial models, along with individual nest attributes, help to clarify why populations and breeding success may have fallen in concert with changing lake levels. During the study period (2013-2020), the Great Lakes, which includes the St. Clair Flats region, experienced record-breaking lake-level rise. The 2013 annual

average lake level in Lake St. Clair was 174.82 m, or 0.21 m below-record average (1918 to present). After 2014, levels rose above the record average and by 2020 reached an annual average of 175.85 m (*20*). The resulting loss of favorable habitat, which was clearly visible in the geospatial outputs, appeared to force black terns to nest in deeper water, closer to the main lake, and/or attempt nesting in sites with higher ratios of dense vegetation. As lake levels rose at most sub-colonies, so did the extent of open water, while dense vegetative stands remained relatively the same. The areas which suffered the greatest losses were the patchy *Schoenoplectus* sp.- and *Typha* spp.-dominated regions that supported hatching success probabilities greater than 50%. As expected, the area with >50% hatching probability was a significant predictor of black tern sub-colony population size in our mixed model. In the St. Clair Flats region, which contains abundant open water for foraging, the limiting factor for black terns appears to be dispersed emergent vegetation for weather protection, predator concealment, and producing and containing an adequate amount of nest-building materials (*33*, *35*, *38*, *39*).

The relationship between lake levels and black tern nesting survival appears to be predominantly influenced by how well the wetland can maintain a stable extent of safe habitat under the stress of successional barriers and shifting lake levels. Under natural circumstances, marsh communities are adapted to adjust to lake level variations, and are likely better at surviving extreme hydrological swings. Native marsh communities respond to lake level change by migrating lakeward during receding lake levels, and advancing shoreward as they rise, provided the condition in either direction is habitable (e.g., hydric soil condition, water depth, hydrologic energy). However, increased "hardening" of the shoreline through human developments (e.g., housing, seawalls) prevents shoreward advance of marshland communities during high lake levels. The loss of wetland adaptive capacity due to human development is a pervasive issue not only in the Great Lakes (*62*), but worldwide (*63*). In St. Clair Flats, we observed that despite rising lake levels, the clearly defined and developed coastal margins did not shift (e.g., **Figure 5**). Emergent habitat loss appeared to be further exacerbated by *Phragmites australis* in St. Clair Flats. After low lake levels, especially after 1999, facilitated propagation on shallow and exposed soils (*43*) *Phragmites australis* aggressively expanded along the coastal margin, capable of advancing clonally in submerged soils and withstanding a wide range of water depths up to 1.8 m (*17*, *48, 59*). Phragmites monocultures blocked shoreward expansion of patchy emergent *Schoenoplectus* sp. and *Typha* spp. dominant communities **(Figure 1)**. As a result, this emergent marsh habitat was inundated at the deeper end of their distribution, while being unable to replace such losses by advancing into newly flooded shallower zones. The decline in emergent marsh habitat is most obvious in **Figure 5** and resulted in precipitous black tern nesting habitat decline. Simply put, viable black tern habitat was caught between impermeable landward barriers (e.g., *Phragmites australis,* human developments), and advancing lake levels, consequentially constricting the black tern population to collapse.

Wherever widespread relationships between monospecific invasions, hydrologic lows, and marsh bird habitat have been investigated, it has been important to understand how local context affects a wetlands' adaptability to lake level swings (*22*, *27*, *64*). During the most recent major drought period in the Great Lakes (late 1990's to 2013) (*20*), large-scale studies on a variety of coastal wetlands largely found that black tern and other marsh bird (e.g., American bittern, least bittern, American coot, black tern, sora) populations declined with stable low lake level conditions because these enabled significant encroachment of invasive species (*19*, *22*, *27*)**.** In Green Bay (Wisconsin, US), the levels of Lake Michigan rose after 2013, and had a positive correlation with black tern and marsh bird populations; it is suspected that this occurred because their preferred patchy emergent habitat was revitalized (*34*). However, the study did not address the continued lake level rise following 2017 in which, at least at St. Clair Flats, worsened conditions for black terns. Unlike Green Bay, Lake St. Clair's black tern colony was at its known healthiest population and breeding success rates in 2013 and

2014 and had a negative relationship with rising lake levels throughout the entirety of the study's period. The contrast between locations is likely attributed to how natural (e.g., hydrologic energy, bathymetry), and unnatural (e.g., human development, invasive species, dredging) context heavily influences the wetland's elasticity to lake level extremes. The shallow and relatively protected nature of St. Clair Flats may have provided a unique, temporary lakeward refuge for natural hemi-marsh habitat between the late 1990's and 2013, despite considerable *Phragmites australis* encroachment on the exposed shoreline. With rising lake levels, adaptational movement was later heavily restricted by *Phragmites australis* and "hardened", developed shorelines particularly after 2017. Differences in how capable wetlands are of adapting to multi-stressor contexts are important to consider when addressing restoration and protection efforts in an increasingly unstable climate. Variable wetland adaptability also underscores the need for widespread protection and restoration of diverse inland and coastal wetlands in the Great Lakes to buffer and/or prevent periods of habitat inundation and invasion.

Connecting large-scale climate driven variables (lake levels) and local proximate (habitat) variables to nesting success provides important insight towards understanding black tern ecology and conservation strategies, though there is room for improved understanding. The mechanisms tied with nest success and habitat characteristics are still not well understood, and such information has the potential to improve mitigative and restorative approaches. We recommend future monitoring to invest in and utilize remote surveillance methods (e.g., trail cameras) to understand as the impact of mechanisms including predation and wave action. Further, black terns clearly need adequate and stable floating dead plant material or vegetation mounds to nest and this should be further investigated. Unfortunately, we were unable to reliably quantify floating mat extent with the imagery and methods available. Addressing how to classify floating vegetation mats using novel methodology or other remote-sensing tools, such as Synthetic Aperture Radar (SAR), may drastically improve black tern habitat suitability and survivability assessments and is an area of active research.

Wetland restoration is critical for recovering invaluable ecosystem services and diverse, healthy biological populations, including avifauna like the black tern (*14*). The results of our study illustrate how the dynamic effects of climate change (e.g., falling and rising lake levels) generate vastly different habitat scenarios depending on local context (e.g., bathymetry, biodiversity), and stressors (e.g., human development, disturbance, invasive species). Effective restoration will require tailoring to habitat-specific characteristics (*14*) and forecasting the interaction of stressors in multiple climate scenarios (*1*). Many species, including the black tern, can adapt to spatiotemporal variability in wetland habitat via dispersal (*65–67*)**.** However, land cover changes, invasive species, and hydrologic extremes appear to be heavily altering natural turnover of suitable wetlands which support healthy metapopulations (*30*). For the black tern, the North American Breeding Bird Survey found that the number of abandoned colony locations was greater than new establishments between 1966-2013 (*65*). Such long-term assessments indicate that multi-stressor invoked wetland loss is overcoming black terns' adaptation efforts. Recovery of wetland biodiversity will likely require a networked approach, and collaboration to protect and restore large, diverse wetland areas. A higher diversity of protected areas may generate a buffer where species viability is asynchronous and enough suitable wetlands are readily available. The story of Lake St. Clair is a testament to how such local context and/or stressors either 1) prevented habitat loss (shallow, protected river delta) or 2) constricted habitat (landward stressors), during different climate change regimes. Further, it highlights that even the historically largest reservoirs for biodiversity can face collapse during multi-stressor extremes, and we therefore cannot rely on a few major refuges for conservation of wetland species like the black tern. Hope for wetland biodiversity including black terns and other marsh birds in the Great Lakes depends on future widespread knowledge, protection, and restoration efforts to mitigate ongoing climate change, local, and regional stressors threatening their survival.

REFERENCES

1. A. Staudt, A. K. Leidner, J. Howard, K. A. Brauman, J. S. Dukes, L. J. Hansen, C. Paukert, J. Sabo, L. A. Solórzano, The added complications of climate change: understanding and managing biodiversity and ecosystems. *Front. Ecol. Environ.* **11**, 494–501 (2013).

2. C. J. Brown, M. I. Saunders, H. P. Possingham, A. J. Richardson, Managing for interactions between local and global stressors of ecosystems. *PLoS One*. **8**, e65765 (2013).

3. J. A. Orr, R. D. Vinebrooke, M. C. Jackson, K. J. Kroeker, R. L. Kordas, C. Mantyka-Pringle, P. J. den Brink, F. De Laender, R. Stoks, M. Holmstrup, C. D. Matthaei, W. A. Monk, M. R. Penk, S. Leuzinger, R. B. Schäfer, J. J. Piggott, Towards a unified study of multiple stressors: divisions and common goals across research disciplines. *Proc. Biol. Sci.* **287**, 20200421 (2020).

4. R. Dirzo, H. S. Young, M. Galetti, G. Ceballos, N. J. B. Isaac, B. Collen, Defaunation in the Anthropocene. *Science (80-.).* **345**, 401–406 (2014).

5. M. C. Urban, Accelerating extinction risk from climate change. *Science (80-.).* **348**, 571–573 (2015).

6. C. L. Folt, C. Y. Chen, M. V Moore, J. Burnaford, Synergism and antagonism among multiple stressors. *Limnol. Ocean.* **44**, 864–877 (1999).

7. C. M. Crain, K. Kroeker, B. S. Halpern, Interactive and cumulative effects of multiple human stressors inmarine systems. *Ecol. Lett.* **11**, 1304–1315 (2008).

8. M. A. Reid, S. Chilcott, M. C. Thoms, Using palaeoecological records to disentangle the effects of multiple stressors on floodplain wetlands. *J. Paleolimnol.* **60**, 247–271 (2018).

9. Government Canada (U. S. EPA), *The Great Lakes: an environmental atlas and resource book.* (U.S. EPA Great Lakes National Program Office, Chicago, Illinois, third., 1995).

10. A. Trebitz, M. Sykes, J. Barge, A reference inventory for aquatic fauna of the Laurentian Great Lakes. *J. Great Lakes Res.* **45**, 1036–1046 (2019).

11. H. H. Prince, P. I. Paddingi, R. W. Knapton, “Waterfowl use of the Laurentian Great Lakes” (1992), , doi:10.1016/S0380-1330(92)71329-X.

12. Millenium Ecological Assessment, Ecosystems and human well-being: wetlands and water synthesis (2005).

13. P. Meli, J. M. Rey Benayas, P. Balvanera, M. Martínez Ramos, Restoration Enhances wetland biodiversity and ecosystem service supply, but results are context-dependent: a meta-analysis. *PLoS One*. **9**, e93507 (2014).

14. J. C. Brazner, M. E. Sierszen, J. R. Keough, D. K. Tanner, Assessing the ecological importance of coastal wetlands in a large lake context. *SIL Proceedings, 1922-2010*. **27**, 1950–1961 (2000).

15. K. A. Krieger, The Ecology of invertebrates in Great Lakes Coastal Wetlands: current knowledge and research needs. *J. Great Lakes Res.* **18**, 634–650 (1992).

16. M. G. Tulbure, C. A. Johnston, D. L. Auger, Rapid invasion of a Great Lakes coastal wetland by non-native *Phragmites australis* and *Typha*. *J. Great Lakes Res.* **33** (2007), pp. 269–279.

17. N. P. Danz, G. J. Niemi, R. R. Regal, T. Hollenhorst, L. B. Johnson, J. M. Hanowski, R. P. Axler, J. J. H. Ciborowski, T. Hrabik, V. J. Brady, J. R. Kelly, J. A. Morrice, J. C. Brazner, R. W. Howe, C. A. Johnston, G. E. Host, Integrated measures of anthropogenic stress in the U.S. Great Lakes Basin. *Environ. Manag.* **39**, 631–647 (2007).

18. S. J. Bolsenga, C. E. Herdendorf, *Lake Erie and Lake St. Clair handbook* (Wayne State University Press, Detroit :, 1993), *Great Lakes books*.

19. L. Mortsch, J. Ingram, A. Hebb, S. Doka, Great Lakes coastal wetland communities: vulnerabilities to climate change and response to adaptation strategies. *Environ. Canada* (2006).

20. A. H. Clites, J. P. Smith, T. S. Hunter, A. D. Gronewold, Visualizing relationships between hydrology, climate, and water level fluctuations on Earth's largest system of lakes. *J. Gt. Lakes Res.* **40**, 807–811 (2014).

21. A. D. Gronewold, J. Bruxer, D. Durnford, J. P. Smith, A. H. Clites, F. Seglenieks, S. S. Qian, T. S. Hunter, V. Fortin, Hydrological drivers of record-setting water level rise on Earth's largest lake system. *Water Resour. Res.* **52**, 4026–4042 (2016).

22. K. E. Wyman, F. J. Cuthbert, Black tern (*Chlidonias niger*) breeding site abandonment in U.S. Great Lakes coastal wetlands is predicted by historical abundance and patterns of emergent vegetation. *Wetl. Ecol. Manag.* **25** (2017), pp. 583–596.

23. C. D. Robichaud, R. C. Rooney, Long-term effects of a *Phragmites australis* invasion on birds in a Lake Erie coastal marsh. *J. Gt. Lakes Res.* **43**, 141–149 (2017).

24. G. Soulliere, M. A. Al-Saffar, R. L. Pierce, M. J. Monfils, L. R. Wires, B. W. Loges, B. T. Shirkey, N. S. Miller, R. D. Schultheis, F. A. Nelson, A. M. Sidie-Slettedahl, C. M. Tonra, D. J. Holm, "Waterbird habitat conservation strategy-2018 revision Upper Mississippi River and Great Lakes Region Joint Venture" (Bloomington, Minnesota, 2018).

25. D. C. Tozer, Marsh bird occupancy dynamics, trends, and conservation in the southern Great Lakes basin: 1996 to 2013. *J. Great Lakes Res.* **42**, 136–145 (2016).

26. B. G. Peterjohn, J. R. Sauer, Population trends of black terns from the North American Breeding Bird Survey, 1966-1996. *Colon. Waterbirds*. **20**, 566–573 (1997).

27. S. T. A. Timmermans, S. S. Badzinski, J. W. Ingram, Associations between breeding marsh bird abundances and Great Lakes hydrology. *J. Great Lakes Res.* **34**, 351–364 (2008).

28. R. J. Craig, K. G. Beal, The influence of habitat variables on marsh bird communities of the Connecticut river estuary. *Wilson Bull.* **104**, 295–311 (1992).

29. H. A. Kantrud, R. E. Stewart, Ecological distribution and crude density of breeding birds on prairie wetlands. *J. Wildl. Manag.* **48**, 426–437 (1984).

30. M. G. Tulbure, C. A. Johnston, Environmental Conditions Promoting Non-native *Phragmites australis* Expansion in Great Lakes Coastal Wetlands. *Wetlands*. **30** (2010), pp. 577–587.

31. J. M. Hickey, R. A. Malecki, Nest site selection of the black tern in western New York. *Colon. Waterbirds*. **20**, 582–595 (1997).

32. P. G. Novak, Black tern (*Chlidonias niger*). *Migr. nongame birds Manag. concern Northeast. Schneider DM Pence, Eds.). US Fish Wildl. Serv. Corner, MA*, 149–162 (1992).

33. E. H. Dunn, D. J. Agro, Black tern (*Chlidonias niger*). *Birds North Am.* (1995).

34. E. E. Gnass Giese, R. W. Howe, A. T. Wolf, G. J. Niemi, Breeding birds and anurans of dynamic coastal wetlands in Green Bay, Lake Michigan. *J. Great Lakes Res.* **44**, 950–959 (2018).

35. M. W. Weller, C. S. Spatcher, Role of habitat in the distribution and abundance of marsh birds (1965).

36. K. E. Wyman, F. J. Cuthbert, Validation of landscape suitability indices for Black Terns (*Chlidonias niger*) in the U.S. Great Lakes region. *Condor*. **118** (2016), pp. 613–623.

37. A. Golawski, E. Mroz, Differences in nest site characteristics and hatching success in White-winged Tern (*Chlidonias leucopterus*) and Black Tern (*Chlidonias niger*). *Hydrobiologia*. **828**, 1–10 (2019).

38. B.-A. Chapman Mosher, (Dept. of Biological Sciences)/Simon Fraser University (1986).

39. R. D. Bergman, P. Swain, M. W. Weller, A comparative study of nesting forster's and black terns. *Wilson Bull.* **82**, 435–444 (1970).

40. H. Firstencel, thesis, The College at Brockport: State University of New York (1987).

41. S. J. Maxson, J. R. Fieberg, M. R. Riggs, Black tern nest habitat selection and factors affecting nest success in Northwestern Minnesota. *cowa*. **30**, 1–9 (2007).

42. S. M. Laurent, St. Mary's College, Winona, MN (1993).

43. D. A. Wilcox, Response of wetland vegetation to the post-1986 decrease in Lake St. Clair water levels: Seed-bank emergence and beginnings of the *Phragmites australis* invasion. *J. Gt. Lakes Res.* **38**, 270–277 (2012).

44. L. Bourgeau-Chavez, S. Endres, B. Michael, M. E. and Miller, E. Banda, L. Zachary, P. and Higman, P. Chow-Fraser, J. Marcaccio, Development of a bi-national Great Lakes coastal wetland and land use map ssing three-season PALSAR and Landsat imagery. *Remote Sens.* **7**, 8655–8682 (2015).

45. R Core Team, R: A language and environment for statistical computing (2013), (available at http://www.r-project.org/).

46. R. E. Roth, D. Hart, R. Mead, C. Quinn, Wireframing for interactive & web-based geographic visualization: designing the NOAA Lake Level Viewer. *Cart. Geogr. Inf. Sci.* **44**, 338–357 (2017).

47. S. R. Heath, E. H. Dunn, D. J. Agro, in *Birds of the World* (Cornell Lab of Ornithology, 2020).

48. S. K. McFeeters, The use of the Normalized Difference Water Index (NDWI) in the delineation of open water features. *Int. J. Remote Sens.* **17**, 1425–1432 (1996).

49. J. Weier, D. Herring, Measuring vegetation (NDVI & EVI). *NASA Earth Obs. Dispin\'\ivel em http//earthobservatory. nasa. gov/Features/MeasuringVegetation/, site Consult. a*. **15** (2019).

50. C. J. Tucker, P. J. Sellers, Satellite remote sensing of primary production. *Int. J. Remote Sens.* **7**, 1395–1416 (1986).

51. H. Akaike, in *Selected Papers of Hirotugu Akaike. Springer Series in Statistics (Perspectives in Statistics).*, Parzen E., Tanabe K., Kitagawa G., Eds. (Springer, New York, NY, 1998; https://link.springer.com/chapter/10.1007/978-1-4612-1694-0_15), pp. 199–213.

52. A. H. Fielding, J. F. Bell, A review of methods for the assessment of prediction errors inconservation presence/absence models. *Environ. Conserv.* **24** (1997), pp. 38–49.

53. C. M. Perrins, The timing of birds` breeding seasons. *Ibis (Lond. 1859).* **112**, 242–255 (2008).

54. S. Verhulst, J.-A. Nilsson, The timing of birds' breeding seasons: a review of experiments that manipulated timing of breeding. *Philos. Trans. R. Soc. Lond. B Biol. Sci.* **363**, 399–410 (2008).

55. J. Swearingen, K. Saltonstall, Phragmites field guide: distinguishing native and exotic forms of common reed (*Phragmites australis*) in the United States. *Plant Conserv. Alliance, Weeds Gone Wild* (2010).

56. M. Moy, Alarm calls and mobbing behavior associated with predation risk in nesting Black Terns (*Chlidonias niger*) (1995).

57. D. A. Albert, D. A. Wilcox, J. W. Ingram, T. A. Thompson, Hydrogeomorphic classification for Great

Lakes coastal wetlands. *J. Great Lakes Res.* **31**, 129–146 (2005).

58. T. B. Peat, L. F. G. Gutowsky, S. E. Doka, J. D. Midwood, N. W. R. Lapointe, B. Hlevca, M. G. Wells, R. Portiss, S. J. Cooke, Comparative thermal biology and depth distribution of largemouth bass (*Micropterus salmoides*) and northern pike (*Esox lucius*) in an urban harbour of the Laurentian Great Lakes. *Can. J. Zool.* **94**, 767–776 (2016).

59. J. M. Farrell, K. L. Kapuscinski, H. B. Underwood, Fine scale habitat use by age-1 stocked muskellunge and wild northern pike in an upper St. Lawrence River bay. *J. Gt. Lakes Res.* **40**, 148–153 (2014).

60. M. J. Hennen, M. L. Brown, Movement and spatial distribution of common carp in a South Dakota glacial lake system: implications for management and removal. *North Am. J. Fish. Manag.* **34**, 1270–1281 (2014).

61. V. L. Lougheed, B. Crosbie, P. Chow-Fraser, Predictions on the effect of common carp (*Cyprinus carpio*) exclusion on water quality, zooplankton, and submergent macrophytes in a Great Lakes wetland. *Can. J. Fish. Aquat. Sci.* **55**, 1189–1197 (1998).

62. S. M. Wensink, S. D. Tiegs, Shoreline hardening alters freshwater shoreline ecosystems. *Freshw. Sci.* **35**, 764–777 (2016).

63. J. E. Dugan, L. Airoldi, M. G. Chapman, S. J. Walker, T. Schlacher, in *Treatise on Estuarine and Coastal Science* (Elsevier Inc., 2012), vol. 8, pp. 17–41.

64. P. S. Burke, Management plan for the black tern (*Chlidonias niger*) in ontario. *Ontario Manag. Plan Ser. Prep. Ontario Minist. Nat. Resour. (OMNR), Peterborough, Ontario. vi* (2012).

65. J. R. Sauer, J. E. Hines, K. L. Fallon, K. L. Parkdieck, D. J. Ziolkowski, W. A. Link, "The North American breeding bird survey, results and analysis 1966 - 2013" (01.30.2015, Laurel, Maryland, 2014).

66. A. L. Derosier, S. K. Hanshue, K. E. Wehrly, J. K. Farkas, M. J. Nichols, "Wildlife action plan: great lakes marsh and emergent wetlands" (Lansing, Michigan, 2015).

67. K. Johst, R. Brandl, S. Eber, Metapopulation persistence in dynamic landscapes: the role of dispersal distance. *Oikos*. **98**, 263–270 (2002).

APPENDIX

3. Head Count Estimates

Monitoring for population sizes included flushing colony nest areas and counting the number of black terns in the area. These estimates were important for estimating overall populations, changes in the size of sub-colonies, and how many nests were likely to be in the area when nests are confirmed to establish. Towards the end of the breeding season, head counts of fledglings were useful for confirming the success of a sub-colony. Due to the sheer size of SCF, sighting successful fledglings is difficult and likely an underestimation. However, chicks appear to spend time in their natal sub-colony at least within their first week of fledging. Monitoring fledgling success improved in 2019 after extensive fledgling geo-locator tracking by Alex Jahn from Indiana University. Unfortunately, fledgling success in 2020 was believed to be extremely poor, albeit highly accurate, given the low population size that enabled researchers to confidently identify which sub-colonies and nests failed or succeeded. Overall head-count methodology is not considered wholly accurate due to nest failures, re-nests and relocation, and technician error. However, head counts are used to identify how many nests are active in a given sub-colony population, ensuring that all nests are checked or accounted for, and eliminating uncertainty of nests with unknown final status.

4. Estimating Nesting Time Frame

Identifying the starting date of each nest provides important temporal information, especially for identifying seasonal initiation and what changing environmental variables these nests experience (i.e., wind and lake fluctuation). Although some nests were found by chance at a very early stage (i.e. 0 eggs, about to begin laying), most nests were found later during incubation or when they had already hatched. To determine the starting date (whenever possible) we used the following criteria.

Egg Laying Stage. Egg-laying is typically carried out at 1-day intervals, with eggs at this early stage sinking fully when placed in water (*1*). Once the typical 3 egg clutch is completed and/or eggs are no longer fully sinking, nest age estimates are adapted from Hays and LeCroy, 1971 (*2*). These floating stages were determined using a proxy species (Common Tern*, Sterna hirundo*); however this method is also accurate for black terns and has been used in other black tern studies including (*3*). Length of exposed shell above water was also adapted to the smaller width of black tern eggs (21.9-26.1 mm) compared to the common tern (31-34 mm) (*4*) by multiplying the exposed diameter of the common tern with the ratio (0.738) of average common tern (32.5 mm) and black tern (24 mm) diameter.

A2 Table 1. Exposed shell dimensions applied to nest age survey calculation.

Type	Letter Stage	Common Tern	Black Tern
Average width (mm)	NA	32.5	24
Exposed Shell Diameter (mm)	e	15	11
	f	17	13
	g	20	15
	h	21	16
	i	25	18

Chick Stage. When chicks are found, they are typically either assessed visually for age (typically between 0-3 days old) by the researcher, or banded and weighed when they can be safely caught. Chick weight can be used to estimate both bird age and age of the nest, and there are multiple methods that can be used. Regardless of the method, if multiple chicks are weighed from the same nest, the largest chick is used to estimate the nest's age (or the oldest, if a larger chick was measured on a later date from the same nest) as it will estimate the earliest start date. The growth rate of chicks under 10 days of age has been identified in multiple sources (*5*–*7*). Their results indicate a weight gain of 4.18-5.18 grams/day. However, this average growth rate is not linear and varies, depending on their age.

Using the weight of chicks measured at St. Clair Flats (Alex Jahn, pers. comm.), a polynomial growth curve was first produced to more finely estimate chick age and attempt to consider potential temporal changes during development. The slope was first taken from two chicks that were weighed upon hatching and 1 or 2 times following (y = 5.9419x + 8.5508, R Square = 0.8112). This slope was applied to chicks measured 2-3 times for weight to estimate their estimated hatch date (n=10). Their consecutive weights were then plotted against the date and time they were measured. If the time of day was not recorded, the average hour of 11:33 am for chick weighing was applied. A polynomial curve was applied to a scatterplot, which had a greater R-squared than a linear regression (0.947) and accounted for the maximum chick weight in the 60-70 g range. Both the polynomial curve and literature suggest that chick growth is largely sustained within the first 10 days (*5*, *6*, *8*). Therefore, age was not measured once the chick was over 50 grams (under 10 days old). A nest however was still aged if a smaller sibling was located, in which case 1 day was added to the nest's total age assuming the chicks hatched within consecutive days of each-other. The polynomial produced the following estimation, where x was the chick's estimated age (days), and y was the known chick weight (g):

$$x = \frac{78\,077 - \sqrt{6\,833\,555\,209 - 111\,360\,000\,y}}{5568}$$

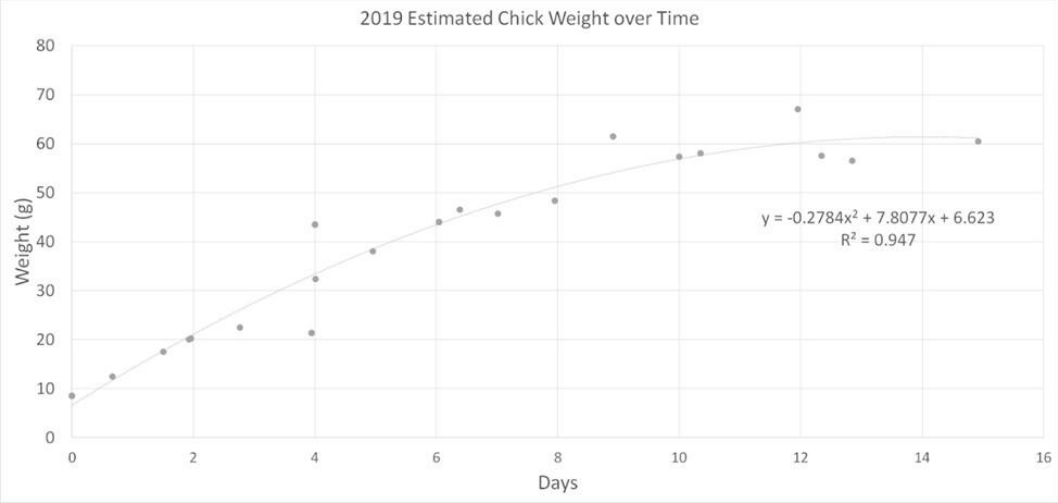

A2 Figure 1. Polynomial curve of estimated chick weight against their age (days) using weights (g) measured 2-3 times per chick; n = 10.

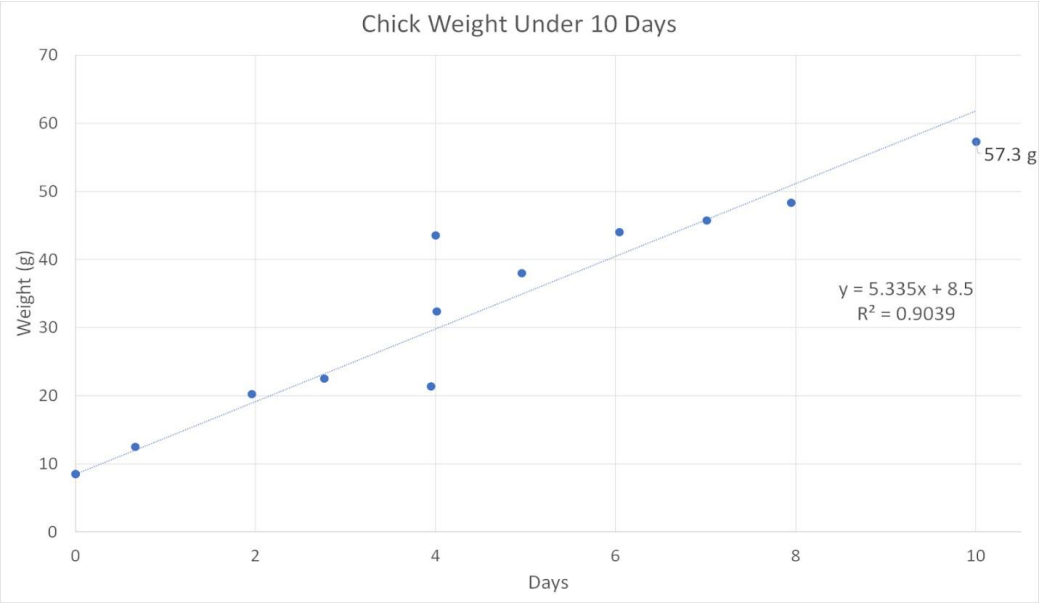

A2 Figure 2. Simplified linear growth of chick against their age (days) using weights (g) measured 2-3 times per chick, under 10 days old; n = 6.

Given the fact that 10 days was the cutoff for accurate age estimation, a simpler, derived linear regression was applied using only weights under 10 days (n = 6). This estimation was slightly higher (5.335 g/day) in comparison to the previously cited studies (4.18-5.18 g/day). If the chicks had fledged, there were some rare circumstances where this information could determine the age of the nest. The observations had to be able to identify "before" and "after" fledging dates and were acquired from a known nest. Chicks are known to fledge between 21 and 24 days of age (*4*). Once chick or fledgling age was successfully estimated, the age of the nest was then calculated by simply subtracting 23 and 24 days (late and early estimates).

The following table summarizes the age estimation methods:

A2 Table 2. Egg age estimation algorithm, adapted from Hays and LeCroy, 1971

Letter	Description	Age Estimate (Days)			
		Young	Midpoint	Old	Error
a0	0 eggs, 1 day prior to laying	0	0	0	0
a1	1 fresh, full sink	1	1	1	0
a2	2 fresh, full sink	2	2	2	0
a	3 fresh, full sink	3	3.5	4	1
b	full sink, slight lift	5	5.5	6	1
c	sink, tilting but not upright	7	7.5	8	1
d	sinking vertically	9	9.5	10	1
e	float, not breaking the surface or 11 mm exposed shell	11	11.5	12	1
f	float, breaking surface (13 mm)	13	13.5	14	1
g	float, breaking surface (15 mm)	15	15.5	16	1
h	float, breaking surface (16 mm)	17	17.5	18	1
i	float, breaking surface (18 mm)	19	19.5	20	1
j	float, breaking surface (18 mm), shell pipped	21	21.5	22	1
k	in process of hatching	23	23.5	24	1
fl	fledged	21	22.5	24	3
	chick growth to fledging + egg incubation + egg laying	44	46	48	4
hatch	chick found and weighed or estimated age visually	age depends on field estimate			varies
	chick age + incubation	add 23	add 23.5	add 24	1

5. Determining Nest Outcome

The following list enumerates (0-8) the possible nest outcomes and how researchers could make this determination:

0 - Unknown egg survival - The nest still had eggs and was clearly active (parents aggressive) on the last date the nest was checked, or, the nest was empty on the last date it was checked and researchers were unable to determine if it failed or hatched. This is likely the case if the nest age and estimated hatch date was unknown, and the area is still active.

1 - Egg fails - The nest was either found with predated eggs, or the eggs were predated or disappeared before it was close to its estimated hatch date. Eggshells or punctured eggs are typically evident of a predator, as adults remove eggshells after hatching.

2 - Egg OR chick fails - The nest was discovered inactive (no aggressive adults in the area), but the date of hatching was unknown, so researchers could not determine if a chick hatched and failed prior to the visit.

3 - Chicks hatched, survival unknown - The nest was discovered with chicks at the nest. Sometimes nests could be deemed "hatched" with reasonable evidence without a chick spotted, if the nest had poop, feathers, and highly aggressive adults.

4 - Some chicks fail, rest are unknown – This is the case is a deceased chick was found at a nest.

5 - All chicks fail - The nest was rechecked after a known hatch, and no chicks or aggressive adults were present in the area. This is rarely a determinable outcome as chicks are capable of swimming away from the nest within days of hatching, and families are known to move their location over time. However, families are unlikely to move significant distances until chicks have fledged (21-24 days). Accurate head counts of the area can provide evidence on whether the parents and chicks are still active in the sub-colony region (i.e., remaining adult pairs in the known area have incubating nests elsewhere).

6 - At least 1 chick fledged - A nest with monitored chicks had a successfully fledged chick which was spotted in the same area and fledged in the correct time period given the age of the chick/nest. Or, in another very rare case, an almost-fledged chick is located near an old nest and a fledgling is spotted in the same area within the same week – without any reason to believe it came from elsewhere. It is extremely rare to encounter this without frequent monitoring and nano-tagging of chicks, which was carried out by Dr. Alex Jahn (2019). Even then, only 4 monitored nests from all years had confirmed fledglings given the almost impossible task of tracing their origin. Nest and chick ages and a firm understanding of the ages of nearby nests must be obtained in order to accurately determine where a spotted fledgling came from.

7 - At least 1 chick fledged and at least 1 sibling failed - A rare occurrence that was encountered only during frequent monitoring of chick survival and fledging by Dr. Alex Jahn (2019)

A3 Table 3. Survival codes 0-8 simplified into egg survival with their associated sample size.

Survival Code	Original Codes	Count	Egg Survival
0	0, 2	370	unknown/egg or chick failed
1	1	165	failed
2	3, 4, 5, 6, 7	286	hatched

6. Water Depth Data Collection

The depths of the lake below individual nests were infrequently collected, with only samples taken in 2018, 2019, and 2020 and even then, only to varying amounts. In many cases, getting close enough to the nest to take this measurement would disturb the nest too much and can cause destruction of the surrounding mat, especially in later years when the lake level was high. However, as an alternative we used the NOAA Lake Level Viewer Tool. This offers an open-source download of a high-resolution (3 m) DEM created by the NOAA Office for Coastal Management using topobathy lidar and dredge survey data (USACE), and multibeam sonar (NPS) (*9*). The "sample" function in ArcMap was used to derive elevation (nearest neighbor) for as many nests as possible from the NOAA DEM and nest GPS locations.

The HECWFS dataset (*10*) was used to derive the water depth (cm) below the nest by subtracting the DEM values from the average HECWFS surface lake level across the nesting (St. Clair Flats) region. For all nests, the depth date was standardized to the onset of the season (5/15). The use of HECWFS and nest DEM was also compared to field depth measurements. This was performed by taking the average 24-hr lake level from HECWFS or Algonac on the same day the field depth (n = 102) was taken and plotting against one another. Unfortunately, in comparison to field measurements, the R squared value was low (0.0801). However, this is not entirely surprising since the water depth can vary widely in regions immediately surrounding each nest. In this case, bathymetric elevation likely represents the depth in a surrounding 9 square meters of the nest and becomes a metric of the surrounding habitat rather than a singular point of reference at the nest itself. Given these uncertainties regarding the true water depth values directly below the nest, and to improve interpretability, water depth values were converted to relative change in cm with the shallowest value set at 0.

7. Lake Level and Wind Point Locations

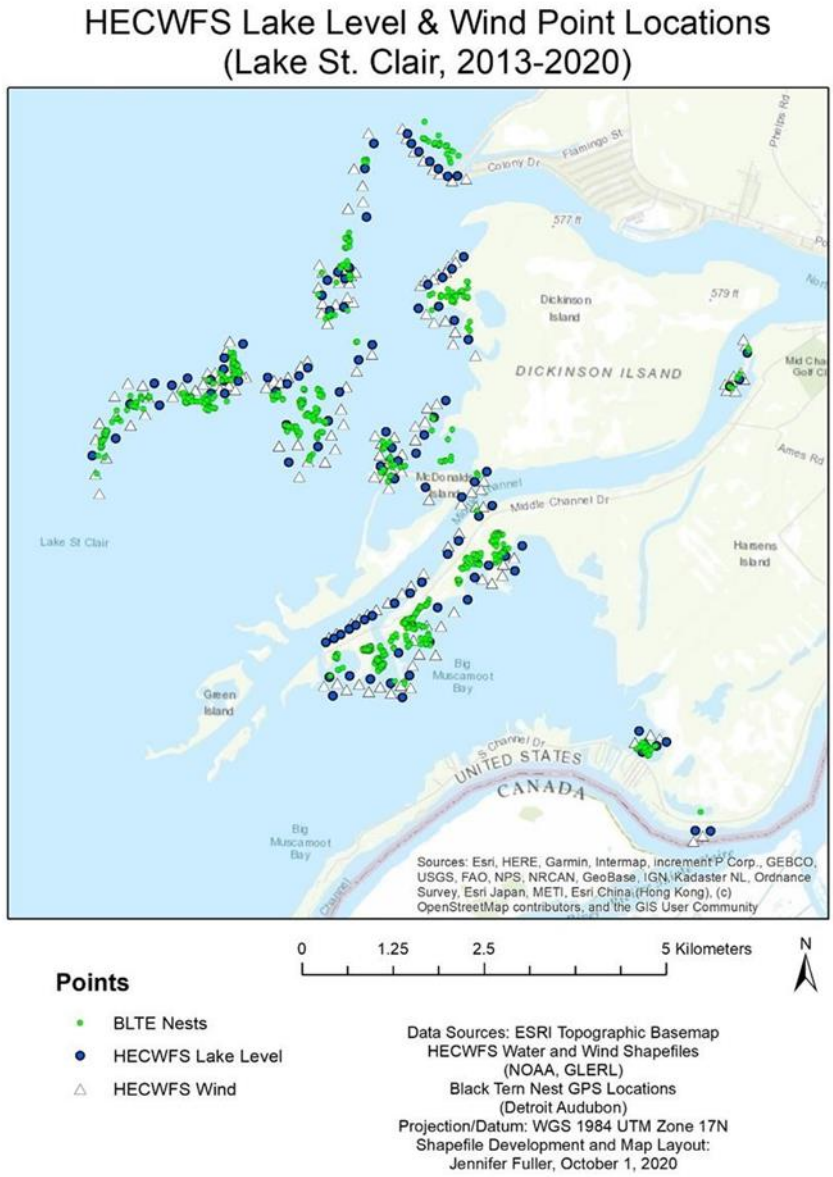

A5 Figure 3. Point locations of nests from all years (2013-2020) in the SCF region, with associated wind and lake level locations where HECWFS 3-hour values are derived. Lake level locations are the same locations in which air temperature values are also collected.

8. Imagery Preprocessing and Collection Dates

4-band, 1 m and 5 m spatial resolution images were collected from multiple sources for geospatial habitat measurements. Images with 1 m spatial resolution were used in to capture fine scale vegetation and open water classes. Sources included commercial satellite images (Kompsat-2, Triplesat-3, WorldView-2 and 3), and open-source aerial photographs from the National Agriculture Imagery Program (NAIP).

All images expect Kompsat-2 were obtained geometrically preprocessed. Kompsat-2 was geometrically corrected at 1:5000 to 1 m resolution (1st Order Polynomial), geometrically corrected NAIP 2016 image. 2013, 2017, and 2019 images were pansharpened using the Brovey method in ArcMap.

Kompsat-2, Worldview-2, and Worldview-3 image bands were individually converted to at-sensor radiance (W m-2 sr-1 µm) and top of atmosphere reflectance (TOA). Dark object subtraction was then performed to control for reflectance variations between different times. Methodology followed procedures, equations, sensor-specific calibration coefficients, and provided metadata detailed in their associated literature.

Kompsat-2 used the following equation and gain/offset values from Lee et al. 2011 (*11*):

$$(1a)\ L\lambda = GAIN \times DN + OFFSET$$

WorldView-2 and WorldView-3 used the same equation described in Comp & Updike 2011, using updated gain and offset values from Kuester, 2017 (*12*). Abscalfactor and effectivebandwith are provided for each band in the imagery metadata:

$$(1b)\ L\lambda = GAIN \times DN \times (abscalfactor/effectivebandwith) + OFFSET$$

To convert to TOA reflectance, all sensors utilized the following relationship:

$$(2)\ p\lambda = \pi \times L\lambda \times d2 / ESUN\lambda \times \cos \theta SZ$$

pλ is band λ TOA reflectance, d is earth-sun distance (astronomical units). ESUNλ is the average band solar exoatmospheric irradiance (W/m2 /µm), values provided for Rapideye-5, Kompsat-2, and WorldView-2/3 using the following references, respectively (*11*–*13*). θSZ is the solar zenith angle calculated by subtracting the solar elevation angle provided in the metadata from 90^{o}.

NAIP imagery was downloaded geometrically and radiometrically corrected. Atmospheric effects were corrected using dark object subtraction based on histograms of each band as described in Chavez, 1988. The Triplesat-3 image was received already radiometrically and atmospherically corrected as a surface reflectance (SR) product.

Unfortunately, images under 1m spatial resolution were limited in temporal availability, particularly when the focal season and habitat changes are occurring within a span of a few months. Therefore, mean NDVI was also used as a more temporally holistic, coarser scale (5 m) proxy of emergent vegetation density. Images for NDVI were collected from Planet as geometrically and atmospherically preprocessed as surface reflectance (SR) products (Rapideye-5 and PlanetScope).

NDVI and NDWI calculations were performed in ArcMap using the built in Image Analysis function and Raster Calculator, consecutively, which utilize the following equations:

$$(1)\ NDVI = (NIR — RED) / (NIR + RED)$$

$$(2)\ NDWI = (GREEN – NIR) / (GREEN + NIR)$$

Commercial and NAIP NDVI and NDWI raster images were then resampled to 1 m resolution; and Rapideye-5 and PlanetScope to 5 m resolution using bilinear interpolation in ArcMap.

Ideally, all images used in NDVI and NDWI analysis would be collected on the same anniversary date each year. Unfortunately, however this is not yet feasible with high-spatial resolution images.

For high spatial resolution imagery, the best compromise was to utilize images as close in timing during the breeding season as possible, and after the advent of "leaf-on" to best differentiate classes. All high spatial resolution images were collected within 9 days of each other (standard deviation = 8.71 days) between late June and July (Table 2). In 2016, visual interpretation and classification of both available images (6/22/2016 and 8/6/2016 dates) showed strong under or overestimation of NDVI values due to the early and late stages in the seasonal growth period. The NDVI raster from 2016 was linearly interpolated between the image from 6/22/2016 and 8/6/2016 to an estimated date of 7/16/2016. This unfortunately assumes a linear relationship in NDVI over time, which is unlikely to be wholly accurate. However, this reduced the standard deviation of dates among years and prevented over or under class estimation bias, which was more desirable than choosing one or the other.

As the temporal resolution was somewhat improved (increasing each year) using PlanetScope and Rapideye-5 (5 m), their NDVI and NDWI raster images were linearly interpolated between the closest two dates to the latest possible date (prior to vegetation senescence) during the nesting season (July 11th) to create anniversary images for comparison.

A6 Table 4. Collection summary table of Planet Imagers (Rapideye-5 & PlanetScope) used for mean NDVI collection including dates, error, original spatial resolution, and source. A stand-in NDVI raster was generated by linearly interpolating between the "Early-End Date" and "Late-End Date", and "Error (Day Spand)" is simply the day span between the two images used to create the interpolated image.

Planet Imagery (5m) Temporal and Spatial Resolutions					
Year	Early-End Date	Late-End Date	Error (Day Span)	Spatial	Source
2013	5/16/2013	7/13/2013	58	5	Rapideye-5
2014	6/21/2014	8/17/2014	57		
2015	7/6/2015	7/23/2015	17		
2016	7/8/2016	7/26/2016	18		
2017	7/4/2017	7/23/2017	19	3	PlanetScope
2018	7/8/2018	7/25/2018	17		
2019	7/11/2019	7/11/2019	0		
2020	7/4/2020	7/25/2020	21		

A6 Table 5. Collection summary table of images with a final pansharpened spatial resolution <1m (KS-2, NAIP, TS-3, and WV-2) used for fine-scale habitat classification and distances. Includes collection dates, multi-spectral spatial resolution, panchromatic spatial resolution, and source by year. FIX 2016 and 2017 (2017 is WorldView-2)

High Resolution (1m) Temporal and Spatial Resolutions				
Year	Date(s)	MS Spatial Res (m)	Panchromatic Spatial Res (m)	Source
2013	7/13/2013	5	1.1	Kompsat-2
2014	7/5/2014	1	NA	NAIP
2015	NA	NA	NA	NA
2016	6/22/2016 8/6/2016	2.8	0.7	TripleSat-3
2017	7/31/2017	2.8	0.7	NAIP
2018	7/18/2018	0.6	NA	NAIP
2019	7/20/2019	2	0.5	WorldView-2
2020	7/7/2020	2	0.5	WorldView-2

A6 Table 6. Pre-processing summary table of images with a final pansharpened spatial resolution <1m (KS-2, NAIP, TS-3, and WV-2) used for fine-scale habitat classification and distances. Includes collection dates, source, atmospheric and normalization correction types, additional processing types, and whether or not interpolation was required by year.

High Resolution (1m) Preprocessing Summary					
Year	Date	Source	Atmospheric & Normalization Correction	Additional Processing	Interpolation
2013	7/13/2013	Kompsat-2	TOA + DOS	Pansharpening (Brovey) & Georectification	N
2014	7/5/2014	NAIP	DOS	None	N
2016	6/22/2016	NA	SR + DOS	Pansharpening (Brovey)	Y
2016	8/6/2016	TripleSat-3	TOA + DOS	Pansharpening (Brovey)	
2017	7/31/2017	NAIP	DOS	None	N
2018	7/18/2018	NAIP	DOS	None	N
2019	7/20/2019	WorldView-2	TOA + DOS	Pansharpening (Brovey)	N
2020	7/7/2020	WorldView-2	TOA + DOS	Pansharpening (Brovey)	N

9. Open Lake Classification.

NDWI classes were simplified to reduce open water "pockets" using an ascending boundary clean function, followed by converting the open water class into a polygon. The polygon was exported such only the main lake polygon was selected, i.e., excluding the "pockets" of open water within primarily vegetated areas. Because high resolution imagery could not be obtained in 2015, the 2016 polygon delineation was used. 2016 was chosen as an appropriate representative due to the nominal differences in mean surface lake level between years (175.4426 m, 2015; 175.4999 m, 2016) during the nesting season (May 15th – July 28th) (*10*).

10. GLM Map Model Application

Using the focal statistics tool, each year's NDVI layer was converted so that every grid cell represented the average surrounding NDVI within a circular 7-m radius. The Euclidean distance tool was used to create a continuous raster where each cell represented distance to the main lake and housing. For percentages of thick vegetation, raster images were first re-classed, so the thick vegetation class was equal to 1, and the surrounding area equal to 0. The focal statistics tool then calculated the sum for each cell within a 7-m radius and was rescaled from 0 to 100 to reflect percentage values. Prior to running the GLM and GIS-based application, normalization of the independent variables was required as their ranges differed significantly. All raster layers and associated continuous predictor variables at each nest were rescaled using min-max feature scaling, or unity-based normalization. To ensure direct compatibility, raster layers from each year were ensured to have the same minimum and maximum value, which were then applied to scaling the nest-specific values.

The probability of a nest failing on a scale of 0 to 1 (p) as an s-shaped curve can be expressed using the equation described in McCullagh & Nelder (*14*), 1989 and Lee & Pradhan, 2007 (*15*):

$$p = (1 / 1 + e^{z})$$

z represents the linear combination which incorporates the output intercept, slope coefficients (b), and independent variables (x) of the logistic regression model:

$$z = \text{intercept} + b_1x_1 + b_2x_2 + b_3x_3 + b_nx_n$$

11. Sub-Colony change in Habitat and # Breeding Adults

Between 2013 and 2020 **(A9 Table 8)**, the average May-July lake level rose 1.03 m and the areas around six sub-colonies on average lost 17.79% of habitat with greater than50% hatching success probability (high-survival) and gained 10.69% uninhabitable open water. Uninhabitable vegetated areas including dry land or marsh vegetation with an NDVI greater than 0.72 declined on average by 1.80%. One outlier to this trend was Mud Lake sub-colony, which gained 7.72% high-survival area, 24.06% uninhabitable vegetation, and lost 36.09% of open water. Mackie S. sub-colony lost the most high-survival area during the sub-colonies' known timeframes (61.97%). The Canoe Hwy. and Bruckner's Island sub-colonies were able to be measured between the third longest time frame (2014-2020) which underwent a lake-level increase of 0.81 m. Canoe Hwy. and Bruckner's Island lost an average of 52.93% of high-survival area, gained 0.08% uninhabitable vegetation, and 38.22% open water.

A9 Table 7. Summary table of years where sub-colonies were surveyed for the number of breeding adults, with associated lake-level (m), # breeding adults, % of classes out of their maximum value, and the Pearson's correlation coefficient (R) between classes and the # breeding adults.

sub-colony	year	lake level (m)	# breeding adults	% Maximum Class Coverage		
				>50% survivability	uninhabitable vegetation	uninhabitable open water
Baltimore S.	2016	175.50	8	100	100	65
	2019	175.97	12	32	76	94
	2020	176.01	2	42	76	100
Bruckner's Isl.	2016	175.50	32	100	0	65
	2017	175.65	14	26	0	87
	2018	175.70	46	53	0	100
	2019	175.97	26	8	0	93
	2020	176.01	0	27	100	96
Canoe Hwy.	2014	175.20	40	100	0	49
	2016	175.50	26	96	26	55
	2017	175.65	36	40	0	63
	2018	175.70	10	49	23	90
	2019	175.97	16	5	100	85
	2020	176.01	8	17	30	100
Doty	2014	175.20	50	97	77	45
	2016	175.50	50	100	80	49
	2017	175.65	55	62	27	62
	2019	175.97	0	18	100	87
	2020	176.01	0	22	96	100
Fisher E.	2019	175.97	14	42	100	89
	2020	176.01	2	100	79	100
Fisher W.	2016	175.50	32	100	84	73
	2017	175.65	14	21	100	75
	2019	175.97	0	9	96	88
	2020	176.01	18	23	67	100
Little Muscamoot W.	2017	175.65	26	83	47	58
	2018	175.70	6	100	47	40
	2019	175.97	8	26	100	75
	2020	176.01	6	28	98	100
Little Muscamoot E.	2017	175.65	14	92	100	57
	2018	175.70	10	100	44	76
	2019	175.97	16	29	45	94
	2020	176.01	3	61	29	100
Mackie S.	2014	175.20	120	100	85	18
	2016	175.50	46	99	100	14
	2017	175.65	42	52	94	38
	2018	175.70	4	23	84	73
	2019	175.97	0	4	87	100
Mud Lake	2019	175.97	22	95	100	92
	2020	176.01	11	100	87	100
South Channel	2018	175.70	20	100	NA	57
	2019	175.97	24	62	NA	65
	2020	176.01	0	61	NA	100
Strawberry	2014	175.20	50	100	34	100
	2016	175.50	31	81	100	97
	2017	175.65	11	11	51	100
Baltimore N.	2016	175.50	4	100	100	55
	2019	175.97	4	21	87	83
	2020	176.01	0	11	78	100

A9 Table 8. Summary table of each sub-colony included in the geospatial analysis for more than 1 year. The change in area with >50% hatching success probability (geospatial model derived), uninhabitable vegetated regions (NDVI > 0.72), and open water are shown with their associated sub-colony, change in lake level, and longest period of change.

sub-colony	Δ lake level (m)	year		percent change		
		start	end	>50% survivability	uninhabitable (dry land or NDVI > 0.72)	open water
Baltimore N.	1.03	2013	2020	-34.15	0.51	28.11
Baltimore S.				-8.34	-20.79	20.92
Doty				-29.60	-8.97	23.03
Fisher E.				-21.87	2.35	9.75
Fisher W.				-20.51	-7.97	18.42
Mud Lake				7.72	24.06	-36.09
Mackie S.	1.00	2013	2019	-61.97	-4.45	56.58
Bruckner's Isl.	0.81	2014	2020	-54.69	0.04	39.95
Canoe Hwy.				-51.17	0.12	36.50
Strawberry	0.67	2013	2017	-15.68	-2.48	-0.67
Little Muscamoot W.	0.51	2016	2020	-46.85	1.94	29.94
Little Muscamoot E.				-34.07	-5.48	29.30
North Hwy.	0.36	2017	2019	-26.01	0.00	25.66
South Channel	0.31	2018	2020	-21.77	0.00	21.39

12. Camera footage during storm events

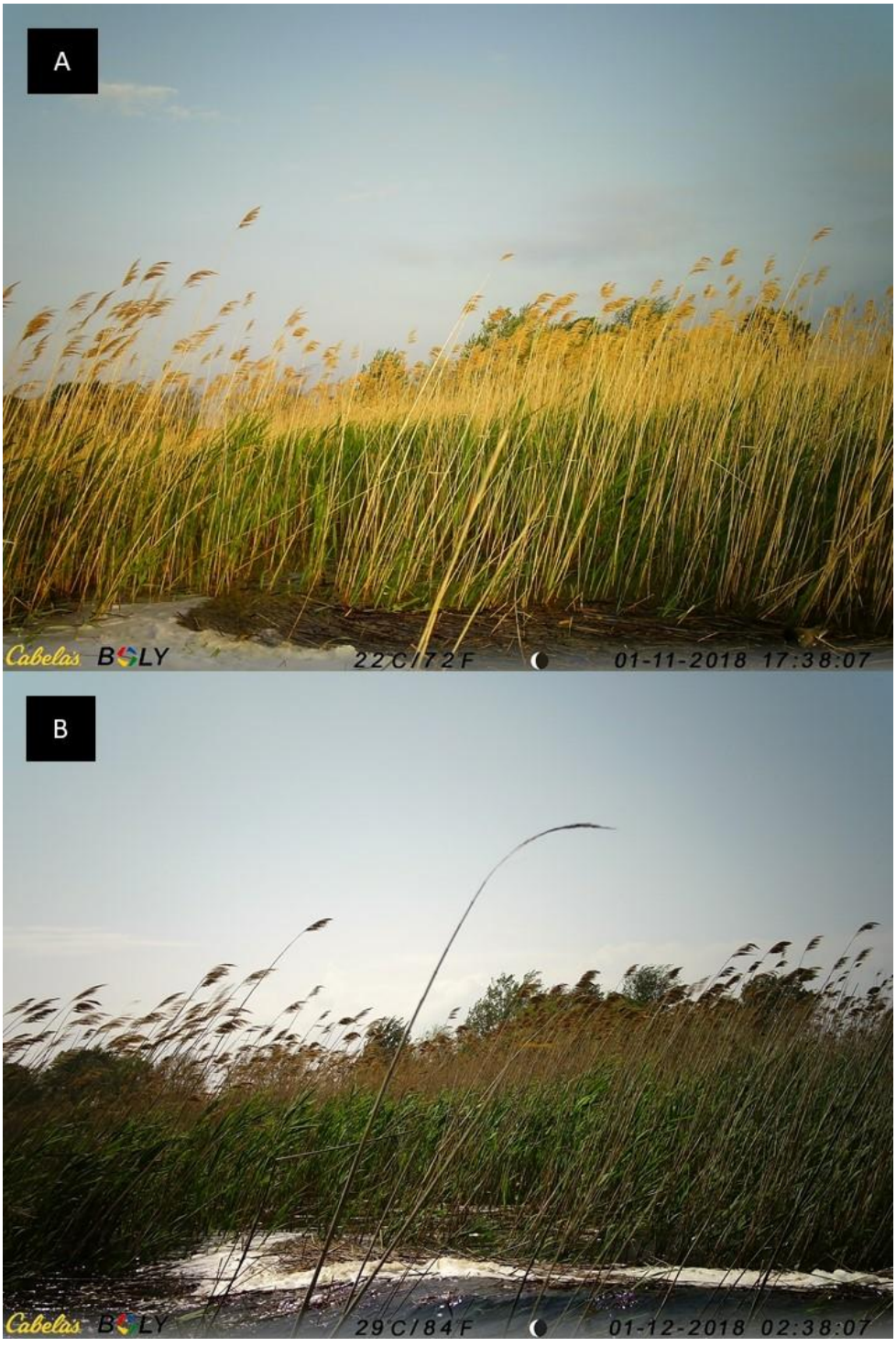

A10 Figure 4. Nest 311 in Little Muscamoot (W) sub-colony against *Phragmites* during A) the day it was last seen and B) a large wave which destroyed the mat. An error occurred in the camera's timestamp recording and actual time after correction are A) 7:10 and B) 16:10 on 6/12/2020.

13. Wind, Lake Level, and Air Temperature Fluctuation (HECWFS)

Surface water levels, air temperature, and wind speeds were collected from the NOAA HECWFS model (*15*) (Anderson, personal communication). HECWFS datapoints were chosen by using the "generate near table" function in ArcMap, collecting the 4 nearest water level/air temperature points and 2 nearest wind points to all nests **(A11, Figure 5).** All the resulting nest GPS locations had associated HECWFS data from each year, regardless of whether the nest occurred. This ensured that the overall weather data was representative of the full nesting region. Raw data was converted from their native, separate `txt` files by point and year to combined excel files by year. Wind data was converted from direction and distance to m/s applying a Pythagorean equation to the two values (North and East). Lake level data remained in its original format as surface elevation (m). The temporal resolution of the HECWFS model is 3 hours. Water and wind data were assigned to sub-colony regions with some overlap and were compared within R for any major differences in fluctuation. Outliers were then removed from each sub-colony, and an average was taken for each sub-colony region. This simplified the data to an appropriate level.

To contextualize these variables in terms of individual nests and their response to climatic events, surface water level, air temperature, and wind speeds were visualized alongside nest survival. Each individual nest was plotted over time against the three weather variables, which included visits and various stages during the monitoring period (incubation, hatch, fail, or fledge stages). Lake level was converted into a moving window which plotted the maximum difference within the past 24 hours, every hour. This maximum difference could be any length of time, so long as it was under the 24-hour period. Because maximum wind speeds were more important than variation, these remained as an unaltered continuous variable. Temperatures were plotted as a 24-hr change.

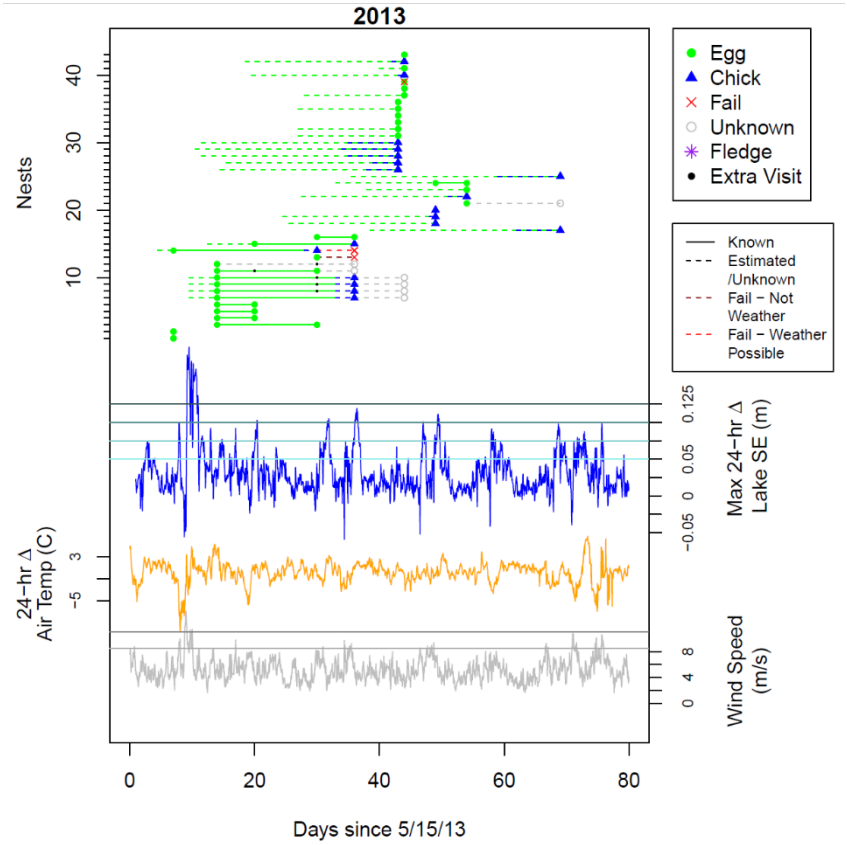

A11 Figure 5. Nest time-frame visualization against mean weather variables collected from the NOAA HECWFS datapoints in the SCF nesting regions. Circles designate a visit confirming incubation of eggs, triangles-chicks, x-failures, open circles-unknown, stars-fledge (a rare occurrence), and small black dots the occurrence of an extra visit. Dashed lines represent estimated or unknown periods. Bold lines are periods of certain, observed nest status. Lake levels are shown as the maximum positive change within a rolling 24-hr window. Air temperature is a rolling change over 24 hours, and wind speeds remain in their native m/s format.

Once the figures were reviewed, the first threshold rise in lake levels under 24 hours was chosen at 5 cm. Particularly in less stormy years (e.g., 2019, 2020), lake level change did not rise over any 24-hrs period much more over this threshold. However according to camera footage and post-storm nest monitoring in 2020, storms at this level were still capable of inflicting damage on some nests. Wind events appeared to have large spikes starting at a threshold of around 8 m/s or 13 mph. This corresponded well to the Beaufort Wind Scale (NERACOOS, n.d.) beginning at Force 5 (*16*). Temperature changes did not appear to spike in accordance with nest loss and was not investigated further.

As an exploratory estimate storm-related failure, nests were categorized as “potentially failed by weather” as long as the nest was not proven to be still active, abandoned, predated, or intact on the last visit, and intersected with a storm event greater than 5 cm in lake level rise or wind speeds over 13 mph or 8.5 m/s. The maximum event a nest survived, if known, could also not be larger than the one that occurred during its failed period. There were considerable assumptions made using these criteria (i.e., variable number of days elapsed between visits, unconfirmed nest destruction by storm), however, the data were not robust enough to apply more stringent filters. The goal of this review was to see if any patterns arise according to weather thresholds, that otherwise would not if failures were only due to randomized events.

Weather data were first filtered to dates where an event occurred over the first threshold of either lake level (5 cm) or wind speed (13 mph). The maximum wind speed or lake level change was then extracted from each of these dates. Each nest was assigned a maximum "survived" event based on the largest event which fell between the nest's estimated start date and last seen active. If the nest did not have an estimated start date, its maximum survived storm was omitted to reduce time frame bias. If a nest failed potentially by weather, a nest was also assigned the maximum weather event that fell between the nest's last seen and last visit.

The datasets were prepared so that nests which survived lake level rise or wind speed over a threshold were assumed to also survive each of the lower thresholds. Failed nests were assumed to fail by the largest event experienced during its failure period. Lake level thresholds were binned at 5 cm intervals, and wind speeds were binned according to the NERACOOS Beaufort Wind Scale.

Unfortunately, storm data was not sufficient to include in the modeling. However, the number of nests to have potentially failed by a storm were compared by threshold. Results of comparisons can be seen in Figure 5 by the percentage of failures per storm size. These figures show potential relationships between the percentage of failed nests and the size of an event (wind or lake level), almost all of which have a positive trend. There appears to be a particular correlation as wind speed increases, which may elude that it is a more important factor when considering causes for physical nest destruction. While nests appeared buoyant during major seiche events at St. Clair Flats, one nest was destroyed due to wind-driven wave action.

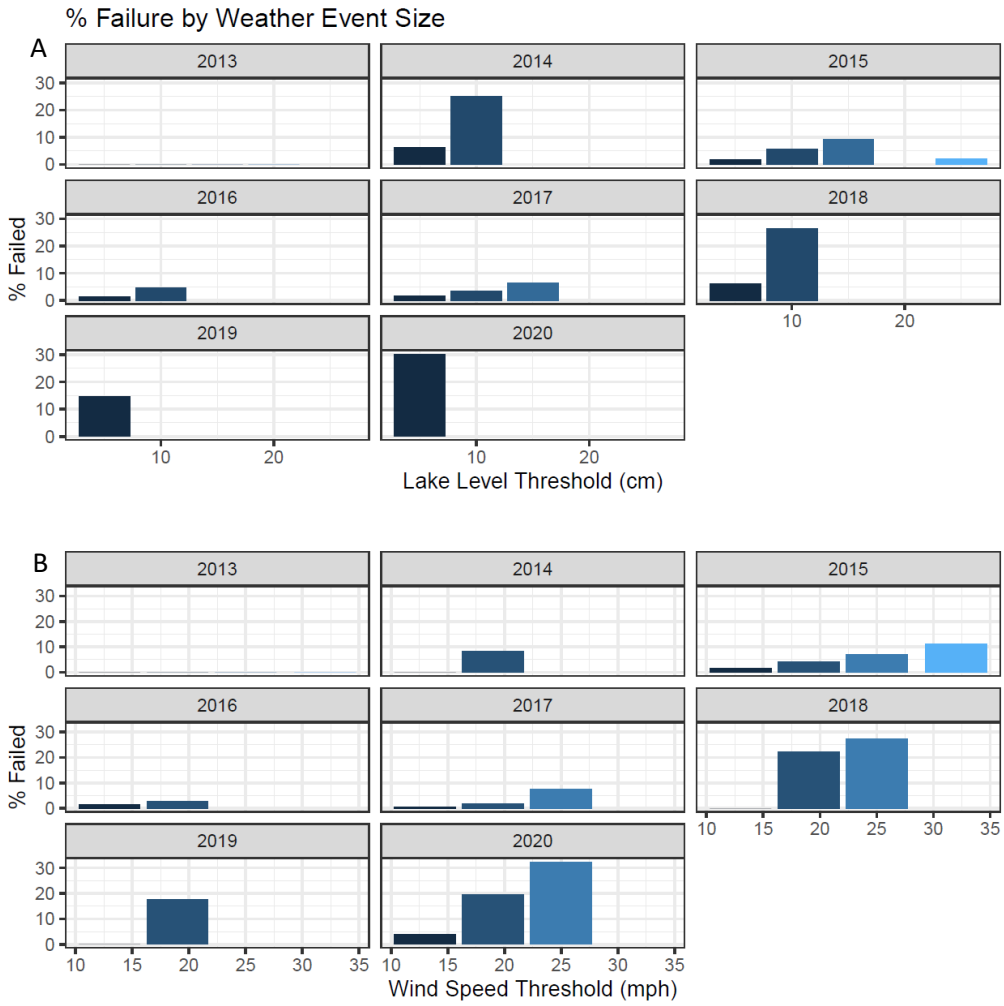

Appx Figure 5. Percentages of failures out of each year's failed nests, sorted by A) threshold lake level or B) wind speed.

REFERENCES (APPENDIX)

1. S. Cramp, Ed., *Chlidonias niger Black tern* (Oxford University Press, Oxford), vol. 4.

2. H. Hays, M. Lecroy, Field criteria for determining incubation stage in eggs of the common tern. *Wilson J. Ornithol.* (1971).

3. V. Von Zuben, J. J. Nocera, Drivers of intra-seasonal variation in black tern (*Chlidonias niger*) nest survival. *Waterbirds*. **42**, 112 (2019).

4. S. R. Heath, E. H. Dunn, D. J. Agro, in *Birds of the World* (Cornell Lab of Ornithology, 2020).

5. E. H. Dunn, Nesting biology and development of young in Ontario black terns. *Can. Field-Naturalist*. **93**, 276–281 (1979).

6. P. F. Bailey, Univ. of Wisconsin Oshkosh.

7. A. T. Gilbert, F. A. Servello, Water Level Dynamics in Wetlands and Nesting Success of Black Terns in Maine. Waterbirds. 28, 181–187 (2005).

8. S. S. Einsweiler, Central Michigan University (1988).

9. R. E. Roth, D. Hart, R. Mead, C. Quinn, Wireframing for interactive & web-based geographic visualization: designing the NOAA Lake Level Viewer. *Cart. Geogr. Inf. Sci.* **44**, 338–357 (2017).

10. A. H. Clites, J. P. Smith, T. S. Hunter, A. D. Gronewold, Visualizing relationships between hydrology, climate, and water level fluctuations on Earth's largest system of lakes. *J. Gt. Lakes Res.* **40**, 807–811 (2014).

11. S. Lee, C. Jin, C. Choi, H. Lim, Y. Kim, J. Kim, Absolute radiometric calibration of the KOMPSAT-2 multispectral camera using a reflectance-based method and empirical comparison with IKONOS and QuickBird images. *J. Appl. Remote Sens.* **6**, 063594 (2012).

12. M. A. Kuester, "Absolute Radiometric Calibration: 2016v0 GE01 and CAVIS."

13. L. Hojas Gascón, G. Ceccherini, F. García Haro, V. Avitabile, H. Eva, The potential of high resolution (5 m) RapidEye optical data to estimate above ground biomass at the National Level over Tanzania. *Forests*. **10**, 107 (2019).

14. P. McCullagh, J. A. Nelder, *Generalized linear models* (Chapman and Hall/CRC, ed. 2, 1989).

15. S. Lee, B. Pradhan, Landslide hazard mapping at Selangor, Malaysia using frequency ratio and logistic regression models. *Landslides*. **4**, 33–41 (2007).

16. Variable Description, (available at http://gyre.umeoce.maine.edu/data/gomoos/buoy/php/variable_description.php?variable=wind_speed).